Investigation into the Role of Binding Loop E on the Function of the Nematode Cys-loop GABA Receptor

by

Ariel D. Kwaka

A Thesis Submitted in Partial Fulfillment

of the Requirements for the Degree of

Masters of Science

In

The Faculty of Science

Applied Bioscience

University of Ontario Institute of Technology

December 2014

© Ariel D. Kwaka, 2014

Certificate of Approval

Abstract

Haemonchus contortus is a parasitic nematode that infects the abomasum of ruminants. While several classes of anthelmintic drugs exist to control nematode infections, *H. contortus* is resistant to all of them. Therefore, novel drug targets such as ligand-gated chloride channels (LGCCs) need to be characterized. The objective of this thesis was to further characterize the agonist binding pocket in Hco-UNC-49BC, the LGCC gated by γ-aminobutyric acid (GABA) within *H. contortus*. To meet this objective, each amino acid residue in binding loop E was changed to a cysteine and analyzed via electrophysiology and the substituted cysteine accessibility method. It was found that of the 18 loop E mutants analyzed, His^{142}, Ser^{144}, Arg^{147}, and Ser^{157}, all played a role in channel activation and were sensitive to modification by a methanethiosulfonate reagent. In addition, mutants lacking His^{142} showed increased sensitivity to a variety of agonists and produced maximal chloride conductance to the previously characterized partial agonist 5-aminovaleric acid. Overall, this thesis has revealed potential differences in the agonist binding pocket between nematode UNC-49 and mammalian GABA receptors that could be exploited in the design of novel anthelmintics.

Keywords: *Haemonchus contortus,* Ligand-gated chloride channel, Hco-UNC-49, GABA, Loop E, Substituted Cysteine Accessibility Method.

Acknowledgements

I want to first thank my supervisor Dr. Sean Forrester who made this Master's thesis a reality. Working in his lab since my undergraduate years, Sean has been a great mentor and very supportive throughout. Secondly, I want to thank my committee members Dr. Janice Strap and Dr. Jean-Paul Desaulniers, who have taught me early on in my education, assisted with my graduate thesis, and have continuously supported me and my professional pursuits. Thirdly, I want to acknowledge UOIT for providing me with a second home since the age of 17, and thank the University for all of the opportunities it has afforded me.

Finally I want to thank my parents and my brother, who kindly sat, smiled, and nodded when I tried discussing my work (as if they knew exactly what I was talking about). Your unfailing care and kind words gave me confidence when I was lacking, and allowed me to give everything I had to my work.

Table of Contents

List of Tables

List of Figures

IMA and DAVA are full agonists for Hco-UNC-49BC H142C mutant. A) Electrophysiology tracings representing maximum response to IMA and DAVA compared to maximal GABA response. B) Dose-response curve analysis of IMA and DAVA compared to GABA. C) Structures of DAVA, IMA, and GABA.

List of Appendices

Amino Acid sequences of Loop E in Hco-UNC-49B and single-cysteine mutants**.** The mutation in each cysteine mutant is represented by a **C**, indicating the substitution of an amino acid to cysteine.

List of Abbreviations

AChBP ……...……Acetylcholine binding protein

Cel-UNC-49……*Caenorhabditis elegans* uncoordinated gene 49

cDNA ……...copy DNA

cRNA……copy RNA

Cys-loop ……...……cysteine loop

[D] ……...…concentration of agonist

DAVA ……5-aminovaleric acid

EC20-50 ……20-50% of maximal effective concentration

EC50 ……...half maximal effective concentration

GABA ……γ-aminobutyric acid

$GABA_A$ ……heteromeric vertebrate GABA-gated chloride channel

$GABA_c$ ……..homomeric vertebrate GABA-gated chloride channel

GluCl ……...glutamate-gated chloride channels

h ……hill slope/coefficient

Hco-UNC-49B .....*H. contortus* uncoordinated gene 49 homopentameric receptor

Hco-UNC-49BC ……*H. contortus* uncoordinated gene 49 heteropentameric receptor

Hco-UNC-49 ……*H. contortus* uncoordinated gene 49

IMA ……..imidazole-4-acetic acid

I_{GABA}.....current elicited from GABA activation of a LGCC

$I_{GABA\text{-}post}$ ……current from GABA activation after MTS application

$I_{GABA\text{-}pre}$ ……...current from GABA activation before MTS application

I_{max} ……maximal current response of agonist

LGCC …….ligand-gated chloride channel

LGIC ……..ligand-gated ion channel

M1-4 ……..transmembrane domains 1, 2, 3, and 4

MS-222 …….3-aminobenzoic acid ethyl ester methane sulphonate salt

MTS ……..methanethiosulfonate

MTSEA …….2-aminoehtylmethanethiosulfonate

MTSET ……2-hydroxyethylthiosulfonate

n ……number of replicates

RDL……..GABA-gated chloride channel in *Drosophila melanogaster*

SCAM ……..Substituted cysteine accessibility method

S.E. …….Standard error

TEVC ……..Two-electrode voltage clamp

Chapter 1: Introduction

1.1 Haemonchus contortus

Haemonchus contortus is a parasitic nematode classified within the same phylum (Nematoda) and clade (V) as the free living model organism *Caenorhabditis elegans* (Blaxter *et al.,* 1998). *H. contortus* consists of morphologically distinct males and females, and reproduces rapidly (Waller & Chandrawathani, 2005). Notorious for infecting the abomasum of ruminating animals such as cattle, sheep, and goats, female *H. contortus* nematodes can produce up to 10,000 eggs per day (Veglia, 1915). The eggs laid in the fourth stomach chamber of the ruminant get passed through the mammal's gastrointestinal system, and are eventually discarded through the feces (Veglia, 1915). Once in the environment two main phases, free-living and parasitic, punctuate the life cycle of *H. contortus* (Nikolaou & Gasser, 2006). *H. contortus* remains free-living until taken up by a host orally, whereby the parasitic life style is adopted upon binding of the nematode to the mucosa layer of the abomasum (Idris *et al.*, 2011).

These gastrointestinal parasites flourish in the host's stomach chamber by extracting and subsequently feeding on blood. By altering the abomasal environment of its host, through the reduction of acid (Simpson, 2000) and disruption of the mucosa (Salman & Duncan, 1984), *H. contortus* may thrive in this environment for an extended period of time, producing the chronic infection haemonchosis (Idris *et al.,* 2011; Waller & Chandrawathani, 2005). Infection from *H. contortus* can ultimately lead to reduced growth, weight loss, severe anemia, and death (Schallig, 2000; Idris et al., 2011).

Referred to as one of the leading causes of morbidity in livestock (Waller *et al.,* 1996; Komuniecki *et al.,* 2012), *H. contortus* infections are a problem all over the world (Prichard, 2001; Waller & Chandrawathani, 2005). Livestock farming suffers great

financial strain as produce is lost to infection, and treatment options cost millions of dollars globally (Waller & Chandrawathani, 2005). As such, *H. contortus* is considered to be one of the most economically significant livestock parasites, bringing the threat of gastrointestinal nematode infections to the fore front of global concern (Waller & Chandrawathani, 2005).

1.2 Anthelmintic Drugs and Resistance

There are three main classes of broad spectrum anthelmintics used for the treatment of parasitic infections, including those caused by *H. contortus*; these drug classes include benzimidazoles, macrocyclic lactones, and imidazolthiazoles (Martin *et al.,* 1997; Ghisi *et al.,* 2007; Williamson *et al.,* 2011). Each of the three drug classes exhibits a unique mode of action, targeting different aspects of the parasite to eliminate the infection. Specifically, benzimidazoles target structural components (β-tubulin) of the cell, while imidazolthiazoles and macrocyclic lactones function by acting as agonists for key receptors in signalling pathways found within the parasite nervous system.

Benzimidazoles, such as thiabendazole, were the first class of anthelmintics introduced to the market in 1963 (Brown *et al.*, 1961; Robinson *et al.,* 1965). Compounds within this drug class exert their effect by specifically binding to the parasite's β-tubulin with high affinity (Martin *et al.,* 1997; Blackhall *et al.,* 2008). Once bound, the drug prevents the polymerization of β-tubulin, an important molecule required for the formation of microtubules within the nematode (Williamson *et al.,* 2011).

Macrocyclic lactones (commonly called avermectins) such as ivermectin, doramectin, and moxidectin, act on anion channels (Martin *et al.,* 1998). Specifically, avermectins are known to agonize and selectively activate invertebrate glutamate-gated chloride channels (GluCl) irreversibly (Martin *et al.,* 1997; Jagannathan *et al.,* 1999; Cheeseman *et al.,* 2001; Yates *et al.,* 2003; McCavera *et al.,* 2009). GluCl receptors, only found in invertebrates (Martin *et al.,* 1997), are similar to other ligand-gated ion channels in structure; the subunits for which have been isolated and characterized within *H. contortus* (Forrester *et al.,* 1999, 2002). Showing a high affinity for binding both ivermectin and moxidectin, continuously activated GluCl receptors are thought to inhibit pharyngeal pumping, likely eliminating the parasite by preventing its ability to feed (Geary *et al.,* 1993; Laughton *et al.,* 1997; Forrester *et al.,* 1999, 2002; Yates *et al.,* 2003; McCavera *et al.,* 2009).

Finally, imidazolthiazoles (also referred to as cholinergic agonists) such as pyrantel, levamisole, and morantel, agonize and selectively activate acetylcholine-gated cation channels found within the somatic muscle of *H. contortus* (Martin *et al.*, 1997, 1998, Neveu *et al.,* 2007). The constantly activated acetylcholine-gated cation channels causes muscle paralysis, allowing the host to eliminate the parasite naturally (Martin *et al.,* 1998).

Extensive use of the aforementioned drugs has resulted in a wide-spread observation of anthelmintic resistance amongst nematodes (Martin *et al.,* 1998; Waller & Chandrawathani, 2005; Williamson *et al.,* 2011). *H. contortus* is prominently cited in drug resistance reports (Waller & Chandrawathani, 2005), and numerous studies have attempted to elucidate the nematode's ability to become resistant to multiple drug classes (Kwa *et al.,* 1995; Sangster *et al.,* 2005; Ghisi *et al.,* 2007; Neveu *et al.,* 2007; Blackhall *et al.,* 2008;

McCavera *et al.,* 2009, Williamson *et al.,* 2011). With respect to benzimidazoles, various point mutations in β-tubulin subunits, such as phenylalanine-200 to tyrosine, has been marked as the main cause of resistance to drugs in this class (Kwa *et al.,* 1995; Ghisi *et al.,* 2007; Blackhall *et al.,* 2008). In this sense, altering the target of the drug is believed to be sufficient to confer the resistance observed. However, there is some indication that higher allele frequencies of P-glycoprotein, a membrane protein capable of transporting drugs out of the cell, may contribute to benzimidazole resistance (Blackhall *et al.,* 2008).

Similar to benzimidazole resistance, various point mutations in GluCl subunits and nicotinic acetylcholine-gated ion channels, were found to be mainly responsible for the resistance to avermectins and imidazolthiazoles respectively (Sangster *et al.,* 2005; Neveu *et al.,* 2007; McCavera *et al.,* 2009). In addition, resistance to the cholinergic agonist levamisole was associated with a down regulation in the number of susceptible receptors expressed, as well as a lack of incorporation of subunits sensitive to the drug (Sangster *et al.,* 2005).

It is clear from the literature that the growing resistance observed in *H. contortus* is becoming a serious concern. Wide spread evolutionary changes occurring in specific drug targets in the parasite have sparked the need for a deeper understanding of nematode neurotransmission, and characterization of unique receptors for future drug design and experimentation.

1.3 Ligand-gated Ion Channels

Ligand-gated ion channels (LGIC) mediate fast chemical neurotransmission once opened by a substrate specific agonist such as a neurotransmitter (Unwin, 1993). Found throughout the nervous system of vertebrates and invertebrates, LGIC control excitatory and inhibitory responses depending upon the channel's permeability to anions (inhibitory) or cations (excitatory). As these channels are involved in the neurotransmission responsible for locomotion and muscle contraction, they are key targets for anti-parasitic drugs and have become the basis for current research (Komuniecki *et al.,* 2012).

Of particular interest is the Cys-loop superfamily of LGICs. Many of the cys-loop receptors are anion-permeable ligand-gated chloride channels (LGCCs), responsible for rapid inhibitory synaptic transmission (Sine & Engel, 2006). LGCCs and other Cys-loop receptors are pentameric membrane proteins, composed of subunits with extracellular (N terminal ligand-binding domain and the C-terminus), intracellular, and transmembrane (M1, M2, M3, M4) domains (Chebib & Johnston, 2000; Jansen *et al.,* 2008; Collingridge *et al.,* 2009) (Figure 1). The central ion pore of LGCCs, through which chloride ions permeate after channel activation, is formed from the transmembrane segment, M2 (Jansen *et al.,* 2008). The characteristic binding loops (A-F) of the receptor are located extracellularly (Jansen *et al.,* 2008).

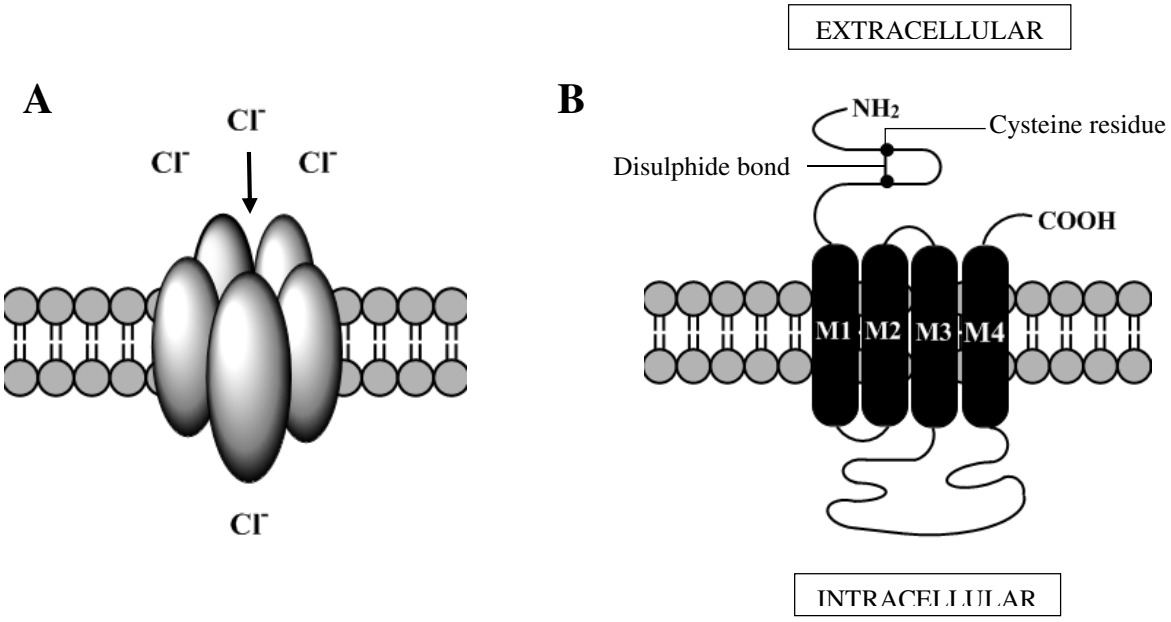

Figure 1. Cys-loop family ligand-gated ion channel structure. A) Schematic of pentameric structure in which subunits arrange to create a pore gated by agonist binding. B) Representative structure of one subunit of a LGIC showing 4 transmembrane regions (M1-M4), intracellular loops, and extracellular loops complete with a disulphide bond connecting two cysteine residues (Adapted from Raymond & Satelle, 2002).

There are many families of LGCCs, in both vertebrates and invertebrates, classified based on the neurotransmitter responsible for opening the channel. However, there are many unique classes of LGCC found in *Caenorhabditis elegans* and *H. contortus*, not found within mammals. This principal alone makes them ideal drug targets for new anti-parasitic pharmaceuticals, as they have the potential to eliminate the parasite without harming the host. These novel nematode LGCCs can be activated by neurotransmitters such as GABA (Siddiqui *et al.,* 2010), glutamate (Cully *et al.,* 1994; Dent, 1997), acetylcholine (Putrenko *et al.,* 2005), and more recently acknowledged biogenic amines, serotonin, dopamine, and tyramine (Rao *et al.,* 2010). The thesis herein focuses on the unique GABA-gated chloride channel in *H. contortus*, referred to as Hco-UNC-49.

1.4 GABA-gated Receptors

Classified as an LGCC, ionotropic GABA receptors share a similar structure with other Cys-loop receptors, and are important for mediating rapid inhibitory neurotransmission in both vertebrates and invertebrates (Cockcroft *et al.,* 1990, Collingridge *et al.,* 2009; Siddiqui *et al.,* 2010). In the vertebrate nervous system, two classes of ionotropic GABA receptors ($GABA_A$ and $GABA_C$) are prominently distributed throughout. The agonist binding pocket of GABA receptors is formed from the interactions of six discontinuous extracellular binding loops (Accardi & Forrester, 2011). Labelled loops A-F, these binding regions bridge to form an interaction between the principle (loops A-D) and adjacent (loops E-F) subunits (Accardi & Forrester, 2011) (Figure 2).

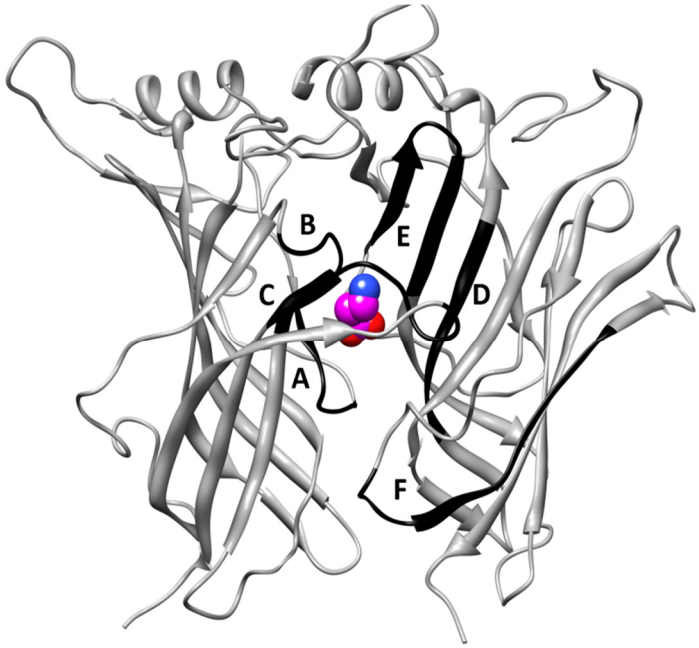

Figure 2. Model of two adjacent Hco-UNC-49B subunits. Binding loops are indicated (A-F) as they interact with a docked GABA molecule (Adapted from Accardi & Forrester, 2011).

These binding loops are present in all of the familial GABA receptors, and have been observed in homology models using the acetylcholine binding protein (AChBP) as a template (Bamber *et al.,* 2003). The presence of the binding loops in multiple GABA receptors may indicate an important conservative feature among them, although there are varying pharmacological profiles of GABA receptors suggesting slight variances that need to be explored.

As mentioned previously, $GABA_A$ and $GABA_C$ are two classes of ionotropic GABA receptors found in the vertebrate nervous system. Within humans, $GABA_A$ receptors serve as drug targets to alleviate insomnia, epilepsy, and anxiety (Sieghart, 1995). The vertebrate genome encodes multiple subunits that assemble in a heteromeric fashion to form $GABA_A$ receptors with varying roles and functions. While the number of subunits and potential pentameric combinations seem endless, subunit expression and strict assembly limit the number of $GABA_A$ receptor subtypes to about a dozen experimentally observed (Bamber *et al*., 2003; Miller & Aricescu, 2014). For example, the human $GABA_A$ receptor subunits include α1-6, β1-3, γ1-3, δ, ε, θ, π, ρ1-3, and while it appears that multiple subtypes can be formed from such a large pool of subunits, the number of physiologically functional channels that form is limited, generally resulting in a configuration of two α, two β, and one γ subunit (Miller & Aricescu, 2014). It should also be noted that $GABA_A$ receptors can assemble into functional homomeric channels, but are not found in discrete populations within the brain (Miller & Aricescu, 2014). Furthermore, the homomeric version of $GABA_A$ receptors have been useful for modelling heteromeric channels, as evidenced by the recent elucidation of crystal structure of the human β3 homopentamer GABA receptor (Miller & Aricescu, 2014).

$GABA_C$ receptors are another class of GABA receptors found within the vertebrate nervous system. These receptors resemble $GABA_A$ receptors, but are classified separately due to their distinct pharmacology and minor variance in structure (Chebib & Johnston*,* 2000; Sedelnikova *et al*., 2005). Unlike $GABA_A$ receptors, $GABA_C$ receptors are slightly simpler in structure, only configured into a homomeric receptor with five identical subunits (Chebib & Johnston*,* 2000). Pharmacologically, $GABA_C$ receptors are uniquely insensitive to bicuculline and can be selectively antagonized by 1,2,5,6-tetrahydropyridine-4-yl-methylphosphinic acid (Sedelnikova *et al.,* 2005). These distinct antagonist profiles indicate that, while structurally similar to $GABA_A$ receptors, these two classes have different agonist/antagonist binding pockets (Sedelnikova *et al*., 2005).

1.5 UNC-49 in C. elegans (Cel-UNC-49)

GABA is an important neurotransmitter in the nervous system of vertebrates as wells as invertebrates; as such, inotropic GABA-gated receptors can be found in both. In invertebrates, GABA receptors are primarily the targets of pesticides and anti-parasitic compounds (Bamber *et al*., 2003). Within the free-living model organism *C. elegans*, the gene *unc-49* encodes for a GABA receptor (Cel-UNC-49) responsible for mediating requisite body muscle inhibition during nematode locomotion (Bamber et al., 2003). The *unc-49* gene has been identified in many free-living and parasitic nematodes (including *H. contortus*), suggesting its importance to GABAergic systems in nematodes (Accardi *et al*., 2012).

Similar to vertebrate GABA receptors, Cel-UNC-49 is a pentameric receptor composed of five subunits. However, unlike the expansive choices of subunits available in

the vertebrate genome, Cel-UNC-49 can only be composed of three possible subunits. The three subunits, UNC-49A, UNC-49B, and UNC-49C, are created through alternative splicing of the *unc-49* gene (Bamber *et al.,* 1999). Through this process, each subunit maintains the same N-terminal ligand-binding domain, but contains a unique C-terminal domain obtained from unique splicing (Bamber *et al*., 1999). Interestingly, pharmacological analysis indicated that subunits UNC-49C and UNC-49B can assemble to form a heteromeric receptor, while UNC-49B can assemble to form a homomeric receptor (Bamber *et al.,* 2003). Upon further analysis of these receptors, it was determined that the homomeric receptor (Cel-UNC-49B) is more sensitive to GABA than the heteromeric channel (Cel-UNC-49B/C), indicating functional differences between the two subtypes (Bamber *et al*., 2003).

Differences between Cel-UNC-49 receptors and mammalian $GABA_A$ receptors were also ascertained by pharmacological analysis. Through experimentation, it was found that unlike vertebrate $GABA_A$ receptors, Cel-UNC-49 receptors are relatively insensitive to bicuculline inhibition or benzodiazepine enhancement (Bamber *et al*., 2003). In order to find structural causation for the differences observed, Bamber *et al*. (2003) compared the sequences of the UNC-49 (UNC-49B, UNC-49C) and $GABA_A$ (α, β, γ) subunits. It was discovered that the *C. elegans* UNC-49 subunits are not orthologous to the $GABA_A$ subunits, but rather closely resemble the GABA-gated RDL receptors found in insects such as *Drosophila melanogaster* (Bamber *et al*., 2003). Despite this, $GABA_A$ receptor subunits and UNC-49 subunits do share similarity in several key structural components (Bamber *et al.*, 2003). Therefore, although UNC-49 receptors are more similar to GABA receptors in other invertebrates, they still share a functional and structural overlap with vertebrate

$GABA_A$ receptors (Bamber *et al.,* 2003). This can be described as a conservation of the GABA receptor family, and knowledge gained from the study of one specific GABA receptor may be applicable, in some way, to all of them.

1.6 UNC-49 in H. contortus (Hco-UNC-49)

UNC-49 in *H. contortus* (Hco-UNC-49) is a GABA-gated chloride channel that has a high degree of sequence similarity, and is orthologous, to UNC-49 in *C. elegans* (Accardi *et al.,* 2012). In addition, Hco-UNC-49 can form heteromeric (assembly of Hco-UNC-49B and Hco-UNC-49C subunits) or homomeric (Hco-UNC-49B only) channels (Siddiqui *et al.,* 2010). While these receptors resemble the assemblage observed in *C. elegans*, the pharmacological implications of the combinatorial subunits differ. In the previous section of the thesis, it was stated that Cel-UNC-49B was more sensitive to GABA than Cel-UNC-49B/C (Bamber *et al*., 2003). In the case of *H. contortus*, the opposite is known to be true (Siddiqui *et al*., 2010). Further study employing cross-species-assembled receptors, those containing both *C. elegans* and *H. contortus* subunits, determined that the Hco-UNC-49B subunit was responsible for the alterations in agonist sensitivity (Siddiqui *et al.,* 2010). These observations suggest that there are functional differences between the two nematode GABA receptors, probably attributed to underlying structural differences.

To begin to elucidate the unique pharmacological profile produced by the Hco-UNC-49 receptor, mutagenesis experiments were conducted (Accardi & Forrester, 2011). Site-directed mutagenesis was performed to determine which residues in loops A-D are required for GABA activation of the Hco-UNC-49 channel. It was found that most of the

residues that are known to play a role in the activation of mammalian GABA receptors, also appear to play a role in Hco-UNC-49. While this study provided some important information of the structure of the nematode GABA receptor, and uncovered important structural links between the binding loops in invertebrates and vertebrates, further studies on the role of amino acid residues in the additional loops E and F, would provide a more complete picture. One such method that could provide a detailed understanding of which residues are involved in agonist binding within the UNC-49 receptor, is a type of mutational technique called the substituted cysteine accessibility method (SCAM).

1.7 Substituted Cysteine Accessibility Method

Traditionally, the role amino acid residues play in the binding and activation of a receptor was determined through the use of site-directed mutagenesis. If the sensitivity of the receptor to its ligand altered when a particular amino acid was mutated, it could be assumed that the residue in question was necessary for the receptor's function. While this approach is still used to this day to indicate which residues are required for function, it does not indicate whether the residue is interacting with the ligand directly (i.e. lining the binding pocket) or indirectly (i.e. needed for structure or allosteric modulation).

Designed to overcome this limitation, Karlin & Akabas (1998) developed the substituted cysteine accessibility method (SCAM). In this analytical technique, the structure and function of the binding site in a receptor is probed through the combination of mutagenesis and chemical modifications. Within this procedure, mutants containing a cysteine residue, in lieu of the residue of interest in the wild-type receptor, are subjected to

applications of thiol specific reagents (methanethiosulfonate derivatives). If the cysteine being analyzed is in an open aqueous environment typical of the agonist binding pocket, the cysteine will be available for modification. The methanethiosulfonate (MTS) reagent will react with the exposed residue, irreversibly modifying and attaching to the cysteine (Newell & Czajkowski, 2007) (Figure 3).

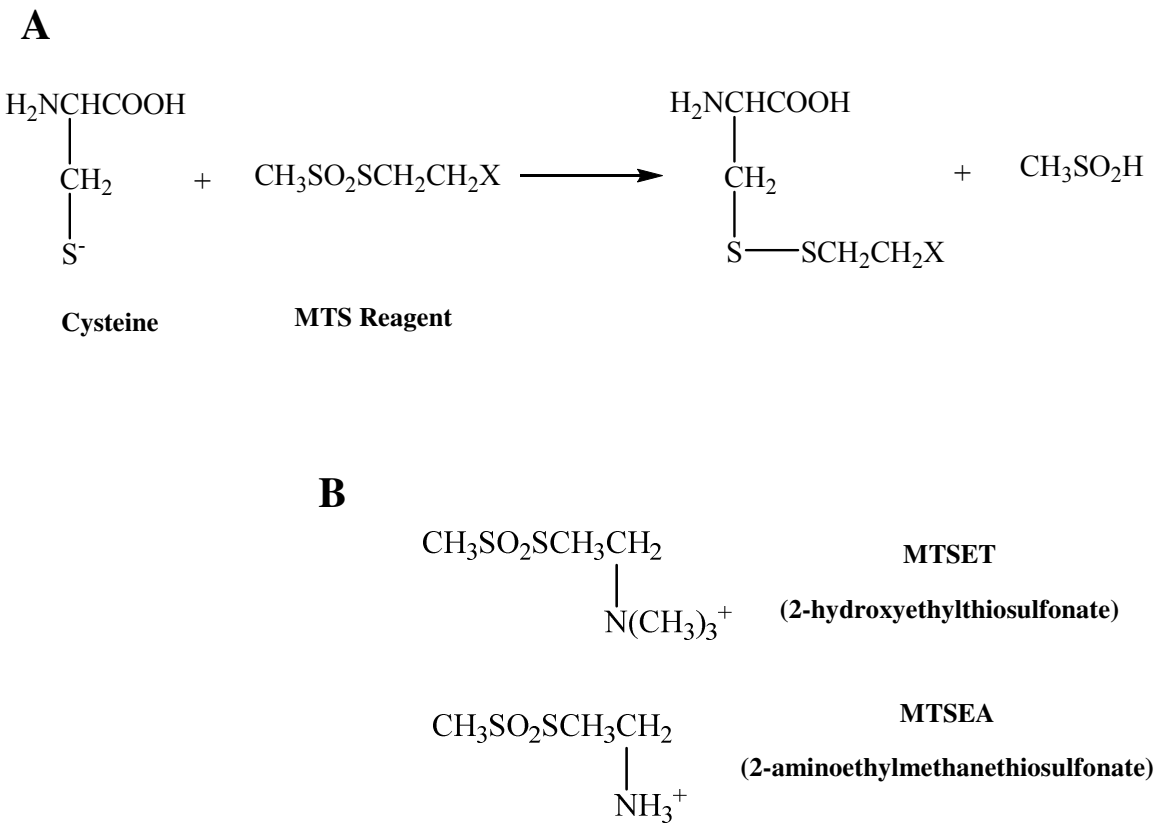

Figure 3. Modification of the sulfhydryl group on a cysteine residue by a methanethiosulfonate (MTS) reagent (A). Structures of two MTS reagents showing side groups (displayed as X in (A)), MTSET and MTSEA (B). (Adapted from Newell & Czajkowski, 2007)

In theory, this modification will block the binding site, thereby altering the function of the receptor, and the sensitivity to the applied agonist. The effect of MTS modification is determined through functional analysis using two electrode voltage clamp electrophysiology on *Xenopus laevis* oocytes expressing the receptor of interest (Newell & Czajkowski, 2007).

When probing the binding site of a receptor, looking for residues that may directly interact with the agonist, two types of experiments are generally performed. The first is a cysteine accessibility test, used to determine if the introduced cysteine is in an aqueous environment. Applying agonist before and after the application of an MTS reagent, the currents elicited are compared (see Newell & Czajkowski, 2007 for more detail). If the amount of activation decreases after MTS application, it can be concluded that the cysteine being analyzed was in an aqueous environment, and accessible for modification by MTS. If the response after MTS application is virtually unchanged, the cysteine residue being examined is most likely imbedded in the receptor, and located in a hydrophobic region of the protein (Newell & Czajkowski, 2007).

While the above technique can be used to determine if a cysteine residue is in an aqueous environment, it cannot determine if this environment is in the binding pocket of the receptor, or if it lies in another aqueous region. Protection assays are used to overcome this limitation. In this technique, low concentrations of the irreversibly reactive MTS reagent is co-applied with a high concentration of agonist. Similar to the cysteine accessibility test, the agonist is applied to the oocyte before and after co-application to determine effects. Since the agonist is of high concentration (EC_{90}-EC_{100}), especially compared to the MTS reagent, it should outcompete MTS for binding in the binding pocket.

If the cysteine residue under analysis lies in the pocket, then the agonist should protect the residue from modification (Newell & Czajkowski, 2007). This protection should allow subsequently applied agonist to activate the receptor at a normal level (Figure 4). If however the cysteine lies outside the binding pocket, the agonist will not be able to block MTS, and therefore full modification of the cysteine by MTS will occur.

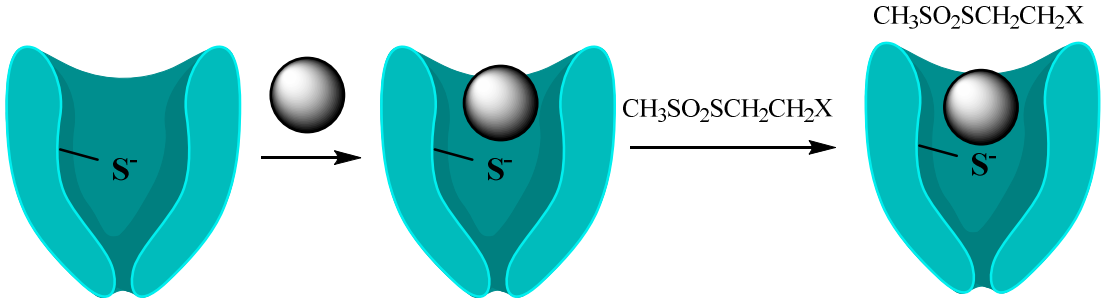

Figure 4. Schematic representation of agonist (gray sphere) protection from the modification of an MTS reagent ($CH_3SO_2SCH_2CH_2X$). Binding pocket, sulfhydryl group, MTS, and agonist not to scale (Adapted from Newell & Czajkowski, 2007).

It should be noted that a cysteine protected by the co-application of agonist may not necessarily be lining the pocket. When an agonist binds, allosteric changes to the conformation of the receptor occurs. In this sense, a cysteine protected by the agonist may either line the binding pocket (i.e. direct protection), or may be hidden from the MTS upon conformational changes (i.e. indirect protection). In such cases, protection assays can be carried out using a competitive antagonist. Covering the same binding pocket as the agonist, but without allosteric modulation upon binding, a competitive antagonist will only protect those residues found directly lining the binding pocket (Newell & Czajkowski, 2007).

1.8 Objectives and Thesis Rationale

According to the aforementioned literature, drug resistance to multiple drug classes displayed by *H. contortus* is a globally expanding problem. Generating a growing need for the identification of novel drug targets, this issue has created an opportunity to garner a deeper understanding of the invertebrate nervous system. As such, more knowledge must be gained about LGIC, the LGCCs, and the structural differences that may account for pharmacological variances observed between vertebrate and invertebrate receptors belonging to the same family.

Expanding on this idea, the following thesis will focus on further characterizing the amino acid residues of Hco-UNC-49, exploring another binding loop not examined before in *H. contortus*. Loop E is a region of the receptor that has been shown to play an important role in agonist binding in other GABA receptors (Sedelnikova *et al.,* 2005; Kloda & Czajkowski, 2007). Furthermore, many of the residues composing loop E have been found to line the agonist binding pocket of vertebrate GABA receptors, and may directly interact with GABA. In 2005, Sedelnikova *et al*. used a combination of mutagenesis and SCAM to locate pocket lining residues situated in loop E of the vertebrate $GABA_c$ receptor subunit ρ1. Using similar techniques, Kloda and Czajkowski (2007) probed loop E of the vertebrate $GABA_A$ receptor subunit α1, also looking for residues that potentially line the agonist binding pocket. In both studies, pocket lining residues were found in loop E ($GABA_A$ α1: N115C, L117C, T129C, and R131C; $GABA_c$ ρ1: V155C, M156C, V159C, S168C, and R170C). While some of the binding pocket residues found in $GABA_C$ were also found in $GABA_A$, there were some residues that were different. It is possible that these unique

residues may explain (at least in part) the differences observed in the pharmacology and receptor kinetics between the two classes of vertebrate GABA receptors.

Due to the similarity in architecture of all ionotropic GABA receptors within the Cys-loop family, it can be assumed that important binding site residues are located in loop E of Hco-UNC-49 as well. However, similar to $GABA_C$, there may be unique residues responsible for GABA activation in Hco-UNC-49. This discovery would advance our understanding of GABA receptors, and the possible causes for the pharmacological variety observed in the GABA LGCC family.

Specifically, the thesis herein will focus on outlining which of the 18 residues within loop E are important for GABA-activation of Hco-UNC-49, and which residues are in aqueous environments, potentially lining the GABA binding pocket. Furthermore, the thesis will describe the uniqueness of the important residues, and how loop E of Hco-UNC-49 compares to its vertebrate counterparts.

Therefore, the objective of this thesis is to use SCAM analysis to probe the residues in binding loop E to determine which are important for the function of the Hco-UNC-49 receptor and which may line the agonist binding pocket.

Chapter 2: Materials and Experimental Methods

2.1 Site-Directed Mutagenesis – Primer Design

Amino acid alignments of *Hco-unc-49b* (Genbank Accession # EU939734.1) and other GABA receptor subunits in the ligand-gated chloride channel (LGCC) family ($GABA_C$ rho-1, $GABA_A$ alpha-1, Cel-UNC-49B, AChBP, etc.), were used to determine the location of loop E within the *H. contortus* sequence (Hco-UNC-49B, $GABA_A$, and $GABA_C$ alignment shown in Figure 5). Located between the histidine residue at position 142 and the leucine residue at 160, primers were designed using Stratagene's web-based QuikChange® Primer Design program (www.stratagene.com/sdmdesigner/default.aspx) to create 18 mutants (H142C, N143C, S144C, F145C, L146C, R147C, I148C, D149C, S150C, D151C, G152C, T153C, V154C, Y155C, T156C, S157C, Q158C, and R159C). Each pair of mutagenic primers (Table 1) were designed to change amino acid residues along loop E into cysteine residues, by way of nucleotide introduction, resulting in singly mutated cysteine mutants (Appendix A).

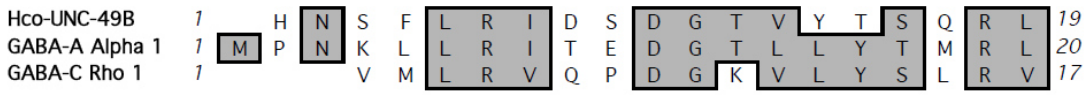

Figure 5. Amino Acid Alignment of Loop E in GABA Receptor Subunits Hco-UNC-49B, $GABA_A$ α1, and GABAc ρ1. Hco-UNC-49B is from *Haemonchus contortus* and shows residues from His^{142}-Leu^{160}. $GABA_A$ α1 is obtained from a rat and demonstrates residues Met^{113}-Leu^{132}. $GABA_C$ ρ1 amino acid sequence is human, and displays residues Val^{155}-Val^{171}.

Table 1. Hco-UNC49B Cysteine Mutagenesis Primers. Each mutagenesis primer name indicates the residue to be mutated, the position of the residue in the Hco-UNC-49B amino acid sequence, and the new residue in the mutant (which is cysteine for all). Mutagenesis primers were designed using Stratagene's web-based QuikChange® Primer Design Program (http://www.stratagene.com/sdmdesigner/default.aspx)

Mutagenesis Primer Name	Forward primer (sense)	Reverse Primer (anti-sense)
H142C	5'-tttccacttggccacaacgtgtaactctttcctgcgaatc-3	5'-gattcgcaggaaagagttacacgttgtggccaagtggaaa-3'
N143C	5'-cacttggccacaacgcattgctctttcctgcgaatcg-3'	5'-cgattcgcaggaaagagcaatgcgttgtggccaagtg-3'
S144C	5'-ggccacaacgcataactgtttcctgcgaatcgac-3'	5'-gtcgattcgcaggaaacagttatgcgttgtggcc-3'
F145C	5'-ccacaacgcataactcttgcctgcgaatcgacag-3'	5'-ctgtcgattcgcaggcaagagttatgcgttgtgg-3'
L146C	5'-ccacaacgcataactctttctgccgaatcgacagcgatggcac-3'	5'-gtgccatcgctgtcgattcggcagaaagagttatgcgttgtgg-3'
R147C	5'-cgcataactctttcctgtgcatcgacagcgatggcac-3'	5'-gtgccatcgctgtcgatgcacaggaaagagttatgcg-3'
I148C	5'-cataactctttcctgcgatgcgacagcgatggcacg-3'	5'-cgtgccatcgctgtcgcatcgcaggaaagagttatg-3'
D149C	5'-ctctttcctgcgaatctgcagcgatggcacggtc-3'	5'-gaccgtgccatcgctgcagattcgcaggaaagag-3'
S150C	5'-cctgcgaatcgactgcgatggcacggt-3'	5'-accgtgccatcgcagtcgattcgcagg-3'
D151C	5'-cctgcgaatcgacagctgtggcacggtctacact-3'	5'-agtgtagaccgtgccacagctgtcgattcgcagg-3'
G152C	5'-gcgaatcgacagcgattgcacggtctacact-3'	5'-agtgtagaccgtgcaatcgctgtcgattcgc-3'
T153C	5'-cgaatcgacagcgatggctgcgtctacactagtcaacgg-3'	5'-ccgttgactagtgtagacgcagccatcgctgtcgattcg-3'
V154C	5'-cgacagcgatggcacgtgctacactagtcaacgg-3'	5'-ccgttgactagtgtagcacgtgccatcgctgtcg-3'
Y155C	5'-cgatggcacggtctgcactagtcaacggc-3'	5'-gccgttgactagtgcagaccgtgccatcg-3'
T156C	5'-cgatggcacggtctactgtagtcaacggcttacg-3'	5'-cgtaagccgttgactacagtagaccgtgccatcg-3'
S157C	5'-ggcacggtctacacttgtcaacggcttacgg-3'	5'-ccgtaagccgttgacaagtgtagaccgtgcc-3'
Q158C	5'-gcgatggcacggtctacactagttgccggcttacggtc-3'	5'-gaccgtaagccggcaactagtgtagaccgtgccatcgc-3'
R159C	5'-ggtctacactagtcaatgccttacggtcaccgcca-3'	5'-tggcggtgaccgtaaggcattgactagtgtagacc-3'

2.2 Site-Directed Mutagenesis of *Hco-unc-49b*

The template used in the site-directed mutagenesis of Hco-UNC-49B was previously sub-cloned into a pT7Ts transcription vector, in which *Xenopus laevis* β-globin untranslated DNA was incorporated into the 5' and 3' ends of the Hco-UNC-49B cDNA (Siddiqui *et al.,* 2010).

A naturally occurring cysteine residue was located at position 224 of the template amino acid sequence, and was removed through site-directed mutagenesis to prevent interference with results obtained from the inserted cysteine residues present in the Hco-UNC-49B mutants. With no alteration in function (Figure 6; Table 2), the cysteine-less mutant (C224A) was used as template, and a baseline from which all data obtained could be compared to throughout the project.

All site-directed mutagenesis performed was conducted using the QuikChange ® Site-Directed Mutagenesis Kit (Stratagene, La Jolla, CA, USA) according to the manufacturer's instructions. Confirmation that the correct mutation was present was verified using DNA sequencing (Genome Quebec).

2.3 cRNA Preparation – *In Vitro* Transcription

Plasmid constructs containing either the mutated *Hco-unc-49b* or wild-type (WT) *Hco-unc-49c* (Genbank Accession # EU049602.1) were linearized and used as template (0.4-1 µg) to create capped *Hco-unc-49* copy RNA (cRNA). The cRNA was made using the mMessage mMachine *in vitro* transcription reaction and the T7 RNA polymerase provided within the transcription kit (Ambion, Austin, TX, USA). cRNA made was

subjected to deoxyribonuclease, precipitated using lithium chloride, and brought to a concentration of 0.5 ng/L upon re-suspension in nuclease free water. Each *in vitro* transcription reaction yielded approximately 10-25 µg of cRNA.

2.4 Expression of Hco-UNC49BC in *Xenopus laevis* Oocytes

Oocytes were obtained surgically from female *X. laevis* (kept in temperature controlled rooms at UOIT; originally received from Nasco, Fort Atkinson, WI, USA), anaesthetized with 0.15% 3-aminobenzoic acid ethyl ester methane sulphonate salt (MS-222; Sigma-Aldrich, Oakville, ON, CA). Lobes of the ovary were extracted, split into smaller pieces of 10-20 oocytes, and defolliculated in a treatment of 2 mg/mL collagenase-II (Sigma-Aldrich) and OR2 solution (82 mM NaCl, 2m M KCl, 1m M $MgCl_2$, 5 mM HEPES pH 7.5) for two hours with gentle rocking at room temperature. After defolliculation, oocytes were stored at 20ºC in ND96 buffer (96 mM NaCl, 2 mM KCl, 1.8 mM $CaCl_2$, 1 mM $MgCl_2$, 5 mM HEPES pH 7.5) supplemented with 100 µg/mL gentamycin and 0.275 µg/mL pyruvic acid (Sigma-Aldrich). Supplemented ND96 solutions were replaced twice every 24 hour period. To reduce the number of operations performed on *X. laevis,* excess ovarian lobes from surgeries were incubated at 4ºC in supplemented ND96 buffer that was replaced once every 24 hours (replacement ND96 chilled to 4ºC). Lobes were prepared and defolliculated after one week of storage as described previously.

Cytoplasmic injections of cRNA were carried out on stage V and VI oocytes using a Drummond Nanoject II (Drummond Scientific Company, Broomhall, PA, USA) assisted

by micromanipulators (World Precision Instruments, Inc., Sarasota, FL, USA). Each oocyte was injected with 50 nL of a mixture of mutated *Hco-unc-49b* and WT *Hco-unc-49c* (equal amounts of 0.5 ng/nL cRNA of each). Electrophysiological recordings were taken after receptor expression, approximately 2-5 days after cRNA injection.

2.5 Two-Electrode Voltage Clamp (TEVC) Electrophysiology

Using an Axoclamp900A voltage clamp (Molecular Devices, Sunnyvale, CA, USA), TEVC electrophysiology was used to observe and record channel activity of Hco-UNC-49BC. Glass electrodes were pulled from borosilicate capillaries using a P-97 Flaming/Brown micropipette puller (Sutter Instruments Company, Novato, CA, USA), and filled with 3M KCl (1-5 MΩ resistance). Each of the two electrodes were connected to Axon Instrument Headstages (Molecular Devices) using Ag|AgCl wires. Oocytes were pierced on either side with the glass electrodes, in which one electrode clamped the oocyte's voltage at -60mV, while the other measured changes to the current caused by activation of the receptor and subsequent channel opening. Compounds used for various analyses utilizing TEVC electrophysiology were perfused over the oocytes through a gravitational flow system into an RC-1Z perfusion chamber (Warner Instruments Inc, Holliston, MA, USA). ND96 buffer was used to dilute the various compounds used, in addition to being used as a wash solution in between drug applications. Recordings and associated data were obtained using Axon Instruments Digidata 1440, Clampex 10.2, and analyzed via Clampfit 10.2 (Molecular Devices).

EC_{50}s were determined for each mutant by perfusing increasing concentrations of GABA (or other agonists) and recording the current observed which included the concentration of agonist that produced maximal current.

2.6 Substituted Cysteine Accessibility Method (SCAM)

Cysteine Accessibility was determined for 10 Hco-UNC-49B mutants (H142C, N143C, S144C, F145C, L146C, R147C, I148C, D149C, S150C, and S157C) as well as the cysteine-less mutant (C224A) using two separate methanethiosulfonate (MTS) reagents. The two MTS reagents used in this project were 2-hydroxyehtylthiosulfonate (MTSET) and 2-aminoethylmethanethiosulfonate (MTSEA), and were obtained from Toronto Research Chemicals (Toronto, ON, CA). During testing, an oocyte was washed and hit with $EC_{20\text{-}50}$ concentrations of GABA in 5 minute intervals until response stabilized within 10%. Once stabilized, either MTSET or MTSEA (1mM for 1 min) was perfused over the oocyte, followed by 5 min of wash with ND96 solution (composition described elsewhere). The $EC_{20\text{-}50}$ concentrations of the mutant being tested was re-applied, and currents were recorded (Sedelnikova *et al.*, 2004, and Kloda & Czajkowski, 2006).

Protection assays were conducted on Hco-UNC-49B mutant H142C and S157C using approximately 100 times the EC_{50} established for the receptor during co-application of GABA (270 µM and 35 mM respectively) and MTSET. The EC_{50} of GABA was used to stabilize the response, and to determine if protection occurred. Standard procedures involved exposing the oocyte to GABA every 5 minutes until current stabilized within 10% of each response, saturated amounts of GABA with MTSET (1 mM MTSET + 100x EC_{50}

GABA for 1 min) were then applied, oocyte was washed for 5 minutes, EC_{50} GABA was re-applied, oocyte was washed for 3 minutes, MTSET (1 mM, 1 min) was applied alone, and GABA EC_{50} was applied again to determine effect.

2.7 Statistical Analysis

Dose-response curves were generated by Prism 5.0 (Graphpad Software, San Diego, CA, USA) using the following equation in the set up log (agonist) vs. normalized response-variable slope:

$$Imax = \frac{1}{1 + \left(\frac{EC50}{[D]}\right)^{h}}$$

Where I_{max} is the maximal response, [D] is the concentration of agonist, EC_{50} is the concentration of agonist that is required to produce half-maximal current, and *h* is the Hill coefficient. Responses used to produce dose-response curves were normalized as a percentage of the maximal current produced by the oocytes individual maximal response to GABA.

The effect of MTS modification was calculated using the following formula:

$$\left(\frac{I_{GABA-post}}{I_{GABA-pre}}\right) - 1$$

Where $I_{GABA\text{-}post}$ is the current produced from GABA activation of the receptor after the application of MTS reagent, and $I_{GABA\text{-}pre}$ is the current produced from GABA activation before the MTS reagent was applied (Kloda & Czajkowski, 2006).

EC_{50} values, *h* values, and standard error (S.E.) were determined using Prism 5.0 from a minimum of three oocytes from two different *X. laevis*. Bar graphs displaying fold changes, comparative currents, and SCAM results were produced from Microsoft Excel 2010. Statistical significance was derived from student t-tests using SigmaPlot 12.5 ($P<0.05$ and $P<0.001$).

Chapter 3: Results

3.1 Characterization of Loop E Cysteine Mutants in Hco-UNC-49BC

The first stage in determining the importance of amino acids residues in loop E of Hco-UNC-49B, to the activation of Hco-UNC-49BC, was to assess their impact on GABA-activation of the channel. Through the use of TEVC electrophysiology, each loop E mutant was exposed to increasing concentrations of GABA for the purpose of determining EC_{50} values. Upon recording, good expressions of all receptors with mutated subunits were observed, all receptors were functional, and clean tracings were obtained (Figure 6A).

Of the 18 mutants tested, 15 showed a significant shift in GABA EC_{50} compared to the C224A cysteine-less mutant from which they were derived (representative dose-response curves are seen in Figure 6B). Of the mutants that displayed a different EC_{50} from C224A (32.56 μM ± 2.29), both H142C and I148C showed an unexpected increase in GABA sensitivity (2.70 μM ± 0.22 and 19.37 μM ± 2.62 respectively). The remaining 13 mutants (N143C, S144C, F145C, L146C, R147C, S150C, G152C, T153C, V154C, Y155C, T156C, S157C, and R159C) had a decrease in GABA sensitivity, with S157C and R159C showing the greatest increase in EC_{50} values (3683.50 μM ± 413.66 and 3102.33 μM ± 130.43 respectively). Finally, three of the cysteine mutants, D149C, D151C, and Q158C, showed no statistical change in GABA EC_{50} ($P<0.05$).

For ease of comparison, the fold change EC_{50} values compared to the EC_{50} of C224A were determined (Figure 7), and all EC_{50} values (±S.E.) with Hill coefficients were calculated (Table 2).

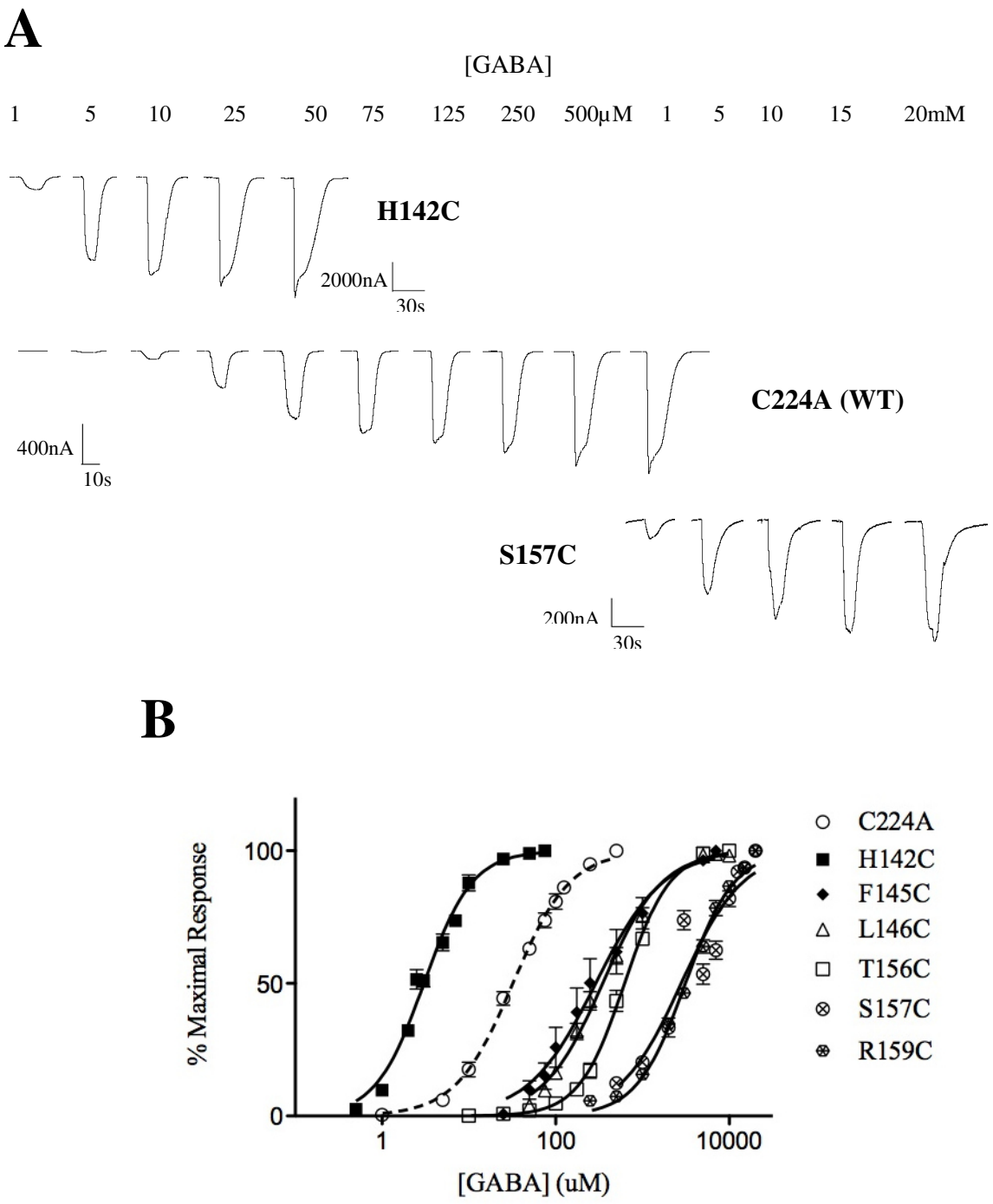

Figure 6. A) Representative electrophysiological tracings of Hco-UNC-49BC with mutated Hco-UNC-49B subunits H142C, C224A (cysteine-less mutant used as template for creation of other mutants), and S157C. B) Dose-response curve of Hco-UNC-49B mutants showing large changes in GABA sensitivity, with normalized currents. Each point represents a mean ± S.E. (n>6).

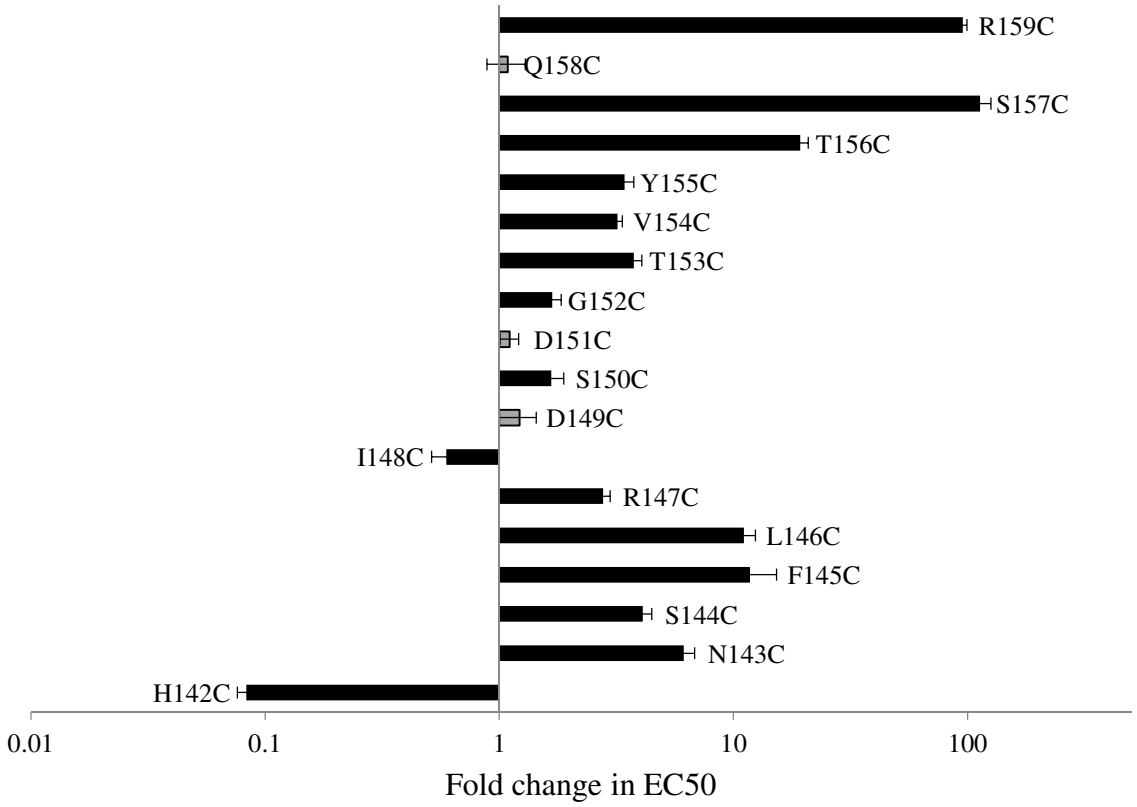

Figure 7. Fold change of EC_{50}, normalized to C224A mutant of Hco-UNC-49B (cysteine-less mutant with WT responses, used as template for creation of other Loop E mutants). Each bar represents a mean of fold change ± S.E. Black bars show statistical significance ($P<0.05$), and gray bars denote no statistical significance. EC_{50} values can be found in Table 2.

Table 2. Comparison of EC_{50} and Hill slope values of Hco-UNC-49B mutants assembled as heteromeric Hco-UNC-49BC receptors, with GABA.

MUTATION	EC_{50} ± S.E. (µM) (*HILL COEFFICIENT* ± S.E.)	NUMBER OF OOCYTES
C224A	**32.56 ± 2.29** (*1.37* ± 0.11)	7
H142C	**2.70 ± 0.22** (*1.44* ± 0.07)	7
N143C	**199.69 ± 22.86** (*1.33* ± 0.11)	7
S144C	**133.76 ± 11.96** (*1.31* ± 0.07)	7
F145C	**383.53 ± 114.30** (*1.40* ± 0.04)	7
L146C	**361.39 ± 42.59** (*1.30* ± 0.04)	7
R147C	**90.32 ± 6.54** (*1.82* ± 0.16)	8
I148C	**19.37 ± 2.62** (*1.53* ± 0.13)	8
D149C	**39.79 ± 7.11** (*2.15* ± 0.27)	7
S150C	**54.39 ± 6.95** (*1.78* ± 0.13)	7
D151C	**36.11 ± 3.25** (*1.43* ± 0.08)	7
G152C	**54.91 ± 5.01** (*1.48* ± 0.06)	7
T153C	**122.21 ± 10.01** (*1.71* ± 0.08)	6
V154C	**104.05 ± 5.10** (*1.51* ± 0.14)	7
Y155C	**111.49 ± 10.68** (*1.64* ± 0.09)	7
T156C	**628.48 ± 50.61** (*1.71* ± 0.06)	6
S157C	**3683.50 ± 413.66** (*1.43* ± 0.09)	8
Q158C	**35.44 ± 6.63** (*1.44* ± 0.10)	7
R159C	**3102.33 ± 130.43** (*1.53* ± 0.03)	6

3.2 Determination of Cysteine Accessibility

Substituted cysteine accessibility method (SCAM) was performed on approximately half of the loop E Hco-UNC-49B mutants made (C224A, H142C, N143C, S144C, F145C, L146C, R147C, I148C, D149C, S150C, and S157C). It was found that out of the 11 mutants tested, only H142C, S144C, R147C, and S157C were modified using MTSET (Figure 8). Furthermore, only S157C had a decrease in % Change in I_{GABA} (-49.75% ± 7.83). Conversely, H142C, S144C, and R147C all showed an increase in % Change in I_{GABA} (88.06% ± 4.02, 38.41% ± 86.60, and 52.51% ± 17.00).

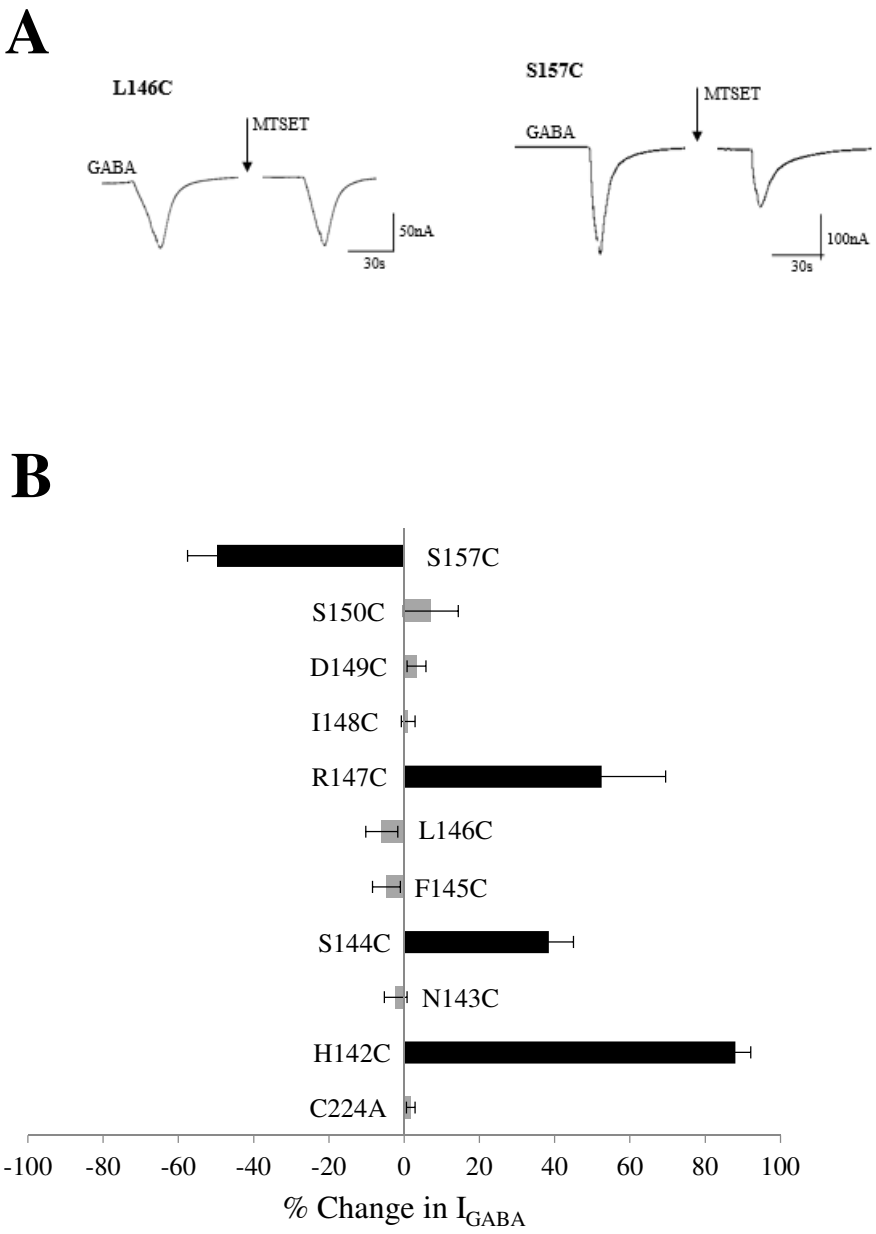

Figure 8. Impact of MTSET on current evoked from GABA activation (I_{GABA}) of Hco-UNC-49BC receptors with mutated Hco-UNC49-B subunits. A) Representative tracings of current elicited from GABA (EC_{20}) before and after MTSET application (1 mM, 1 min). B) Percentage change in current from treatment of mutant Hco-UNC-49BC receptors with MTSET. Each bar indicates the mean ± S.E. (n>3). Black bars denotes statistically significant difference from C224A (P<0.05).

In addition to MTSET, cysteine accessibility tests were performed with MTSEA (Figure 9). Similar trends in % Change in I_{GABA} were observed for S157C, H142C, S144C, and R147C (-73.14% ± 7.14, 76.98% ± 18.20, 34.20% ± 8.92, and 50.30% ± 4.48). However, increased instability of the *X. laevis* oocytes and unexplained reactivity (most likely due to oocyte quality) with the cysteine-less mutant C224A (% Change I_{GABA} = 38.72% ± 27.34) was observed with the use of MTSEA (Figure 9).

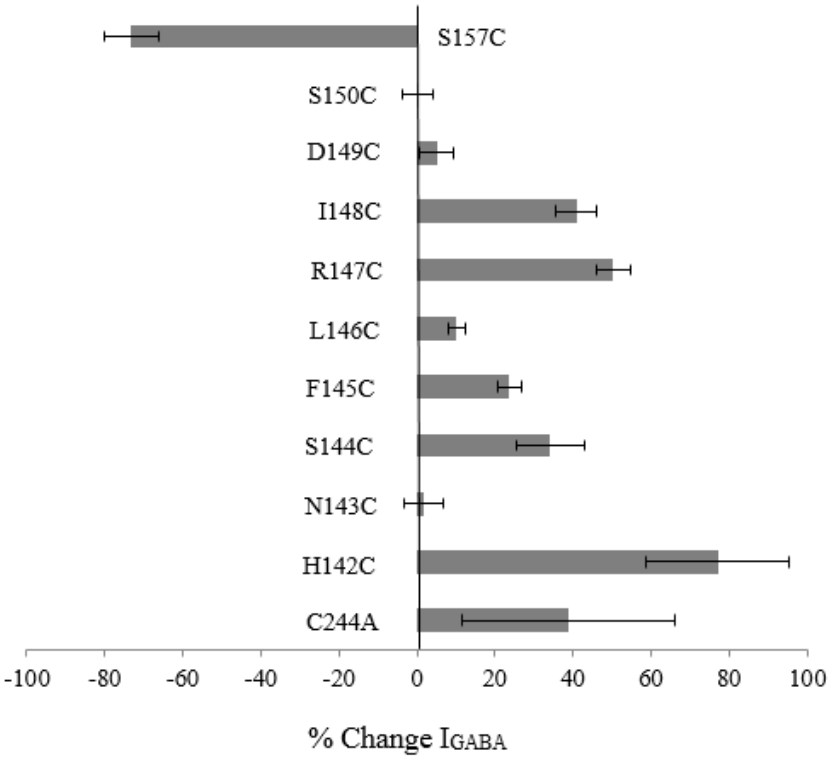

Figure 9. Impact of MTSEA on current evoked from GABA activation (I_{GABA}) of Hco-UNC-49BC receptors with mutated Hco-UNC49-B subunits. Percentage change in current from treatment of mutant Hco-UNC-49BC receptors with MTSEA (1mM, 1min) is displayed. Each bar indicates the mean ± S.E. (n>3).

3.3 Effect of Agonist Binding on Cysteine Modification

Hco-UNC-49B mutants H142C and S157C were analyzed via GABA protection assays. It was determined that H142C was protected to a statistically significant degree (approximately 16.25% difference between MTSET + GABA application and MTSET application alone; $P<0.05$) by GABA (Figure 10). On the other hand, S157C was protected to a small degree (approximately 4.5% difference), but this difference was not found to be significant (Figure 10).

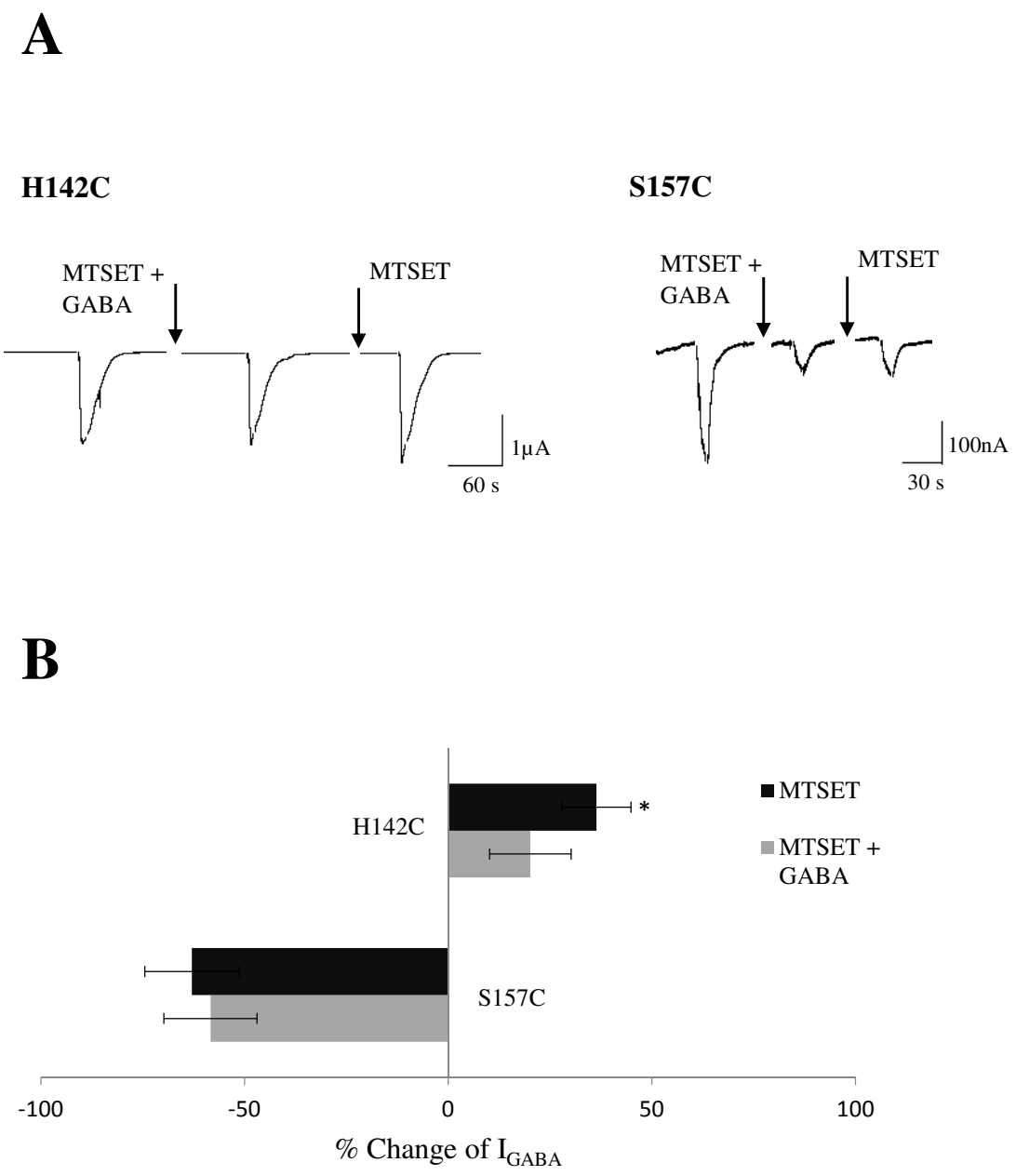

Figure 10. Effects of GABA on MTSET modification of Hco-UNC-49BC Loop E cysteine mutants. A) Representative tracings of currents elicited by EC_{50} GABA on Hco-UNC-49BC (B subunit mutants H142C and S157C), in which arrows represent the application of either MTSET + GABA (100x EC_{50} GABA) or MTSET alone, applied in between EC_{50} GABA hits. B) % Change of I_{GABA} displaying the modification of H142C and S157C with MTSET (black bar) and MTSET + GABA (gray bar). Each bar represents the mean ± S.E. of at least three replicates, and * indicates significant difference ($P<0.05$).

3.4 Further Characterization of H142C Mutant

Upon discovering hypersensitivity to GABA in H142C two other agonists were analyzed, 5-aminovaleric acid (DAVA) and imidazole-4-acetic acid (IMA). EC_{50} values (± S.E.) were determined for both compounds (Table 3) from generated dose-response curves (Figure 11B). From recorded currents, it was determined that both DAVA and IMA act as full agonists on this mutant receptor (Figure 11A), creating maximal currents that were as large as those elicited by maximal GABA concentrations. Finally, by comparing DAVA and IMA EC_{50} values for H142C to Hco-UNC-49BC wild-type, it was found that H142C shows relative hypersensitivity to all of the compounds tested (Table 3).

Table 3. Comparison of EC_{50} and Hill slope values of Hco-UNC-49B mutant H142C (assembled as heteromeric Hco-UNC-49BC receptor) and WT, with IMA, DAVA, and GABA.

Compound	H142C **EC_{50} ± S.E. (µM)** (*Hill Coefficient* ± S.E.)	n	WT[1] **EC_{50} ± S.E. (µM)** (*Hill Coefficient* ± S.E.)	n
IMA	**65.47 ± 6.26** (*1.34* ± 0.13)	6	**174.53 ± 20.75** (*1.93* ± 0.17)	11
DAVA	**1353.2 ± 246.2** (*1.15* ± 0.16)	7	**3914 ± 520** (*1.47* ± 0.18)	7
GABA	**2.70 ± 0.22** (*1.44* ± 0.07)	7	**59.24 ± 7.73** (*2.5* ± 0.42)	9

[1]WT values obtained from MSc. thesis (UOIT) by Mark Kaji, 2012

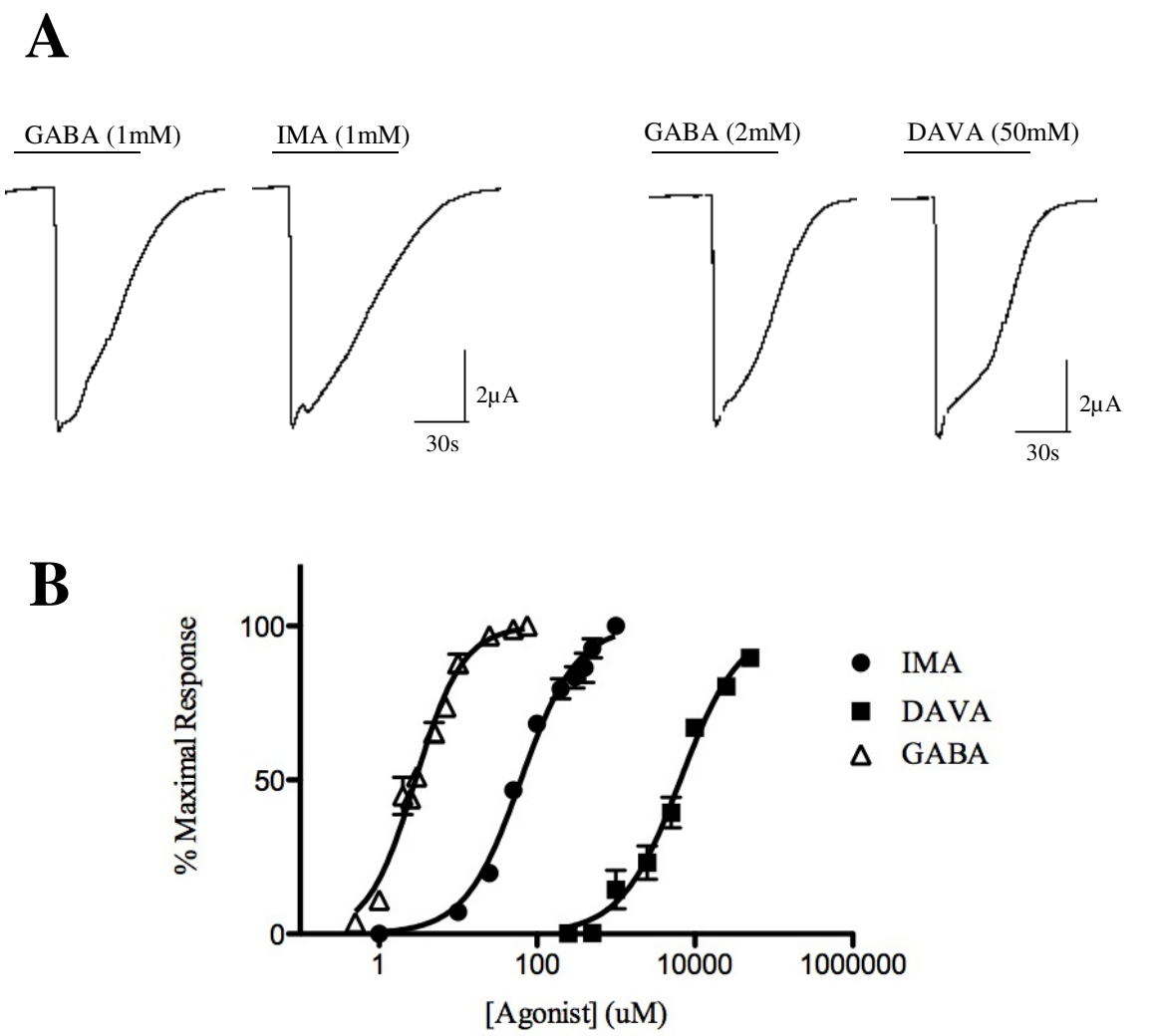

Figure 11. IMA and DAVA are full agonists for Hco-UNC-49BC H142C mutant. A) Electrophysiology tracings representing maximum response to IMA and DAVA compared to maximal GABA response. B) Dose-response curve analysis of IMA and DAVA compared to GABA. C) Structures of DAVA, IMA, and GABA.

Chapter 4: Discussion

This thesis was concerned with characterizing binding loop E in Hco-UNC-49, a GABA-gated chloride channel belonging to the Cys-loop family of receptors. Loop E residues have been shown to line the agonist binding pocket of both $GABA_A$ (Kloda & Czajkowski, 2006) and $GABA_C$ (Sedelnikova *et al.,* 2005) vertebrate receptors, and due to the similarity in structure shared by all receptors in the Cys-loop LGCC family, it stands to reason that residues in loop E of Hco-UNC-49 may also have this role. In order to determine if this was true, residues in loop E were mutated and analyzed for functional effects. Due to time constraints, approximately half of the analyzed mutants were tested to determine if they were in an aqueous environment, and two of these mutants underwent further experimentation to determine if the aqueous environment resides in the binding pocket. Finally, H142C, a hypersensitive mutant, was exposed to additional compounds to further elucidate its role in the function of Hco-UNC-49.

4.1 Hco-UNC-49B Loop E Mutants Effect Functionality of Hco-UNC-49BC

The first objective of this thesis was to determine if residues within loop E of Hco-UNC-49BC are important to the function of the receptor. As stated elsewhere, only 3 mutants (D149C, D151C, and Q158C) did not impact the functionality of the receptor, exhibiting EC_{50} values close to those obtained from C224A (the baseline). From these results, it is believed that the aspartic acid at position 149 and 151, as well as the glutamine at position 158, are not essential for Hco-UNC-49 to function.

The remaining loop E mutants tested, showed a significant difference in their EC_{50} values compared to C224A. Out of all of the mutants analyzed, H142C, S144C, R147C, T153C, S157C, and R159C, produced interesting results.

Within Hco-UNC-49BC, the results seem to suggest that serine at 144 and threonine at 153 are both significant for the receptor to function normally. This was evidenced by the fold change in the EC_{50} values of S144C and T153C compared to the baseline C224A mutant (4.1 ± 0.38 and 3.7 ± 0.31 fold increase respectively). While the fold change may not appear large, the difference was statistically significant ($P<0.05$). This finding is interesting because there was no effect observed when mutating the orthologous amino acid residues at the same positions, in either the $GABA_A$ α1 subunit or the $GABA_C$ ρ1 subunit (Sedelnikova *et al.,* 2005; Kloda & Czajkowski, 2006). The serine at position 144 in Hco-UNC-49B aligns to a lysine in the $GABA_A$ α1 subunit (position 157) and a valine in the $GABA_C$ ρ1 subunit (position 155). Since these three amino acids contain very different properties and overall structures (i.e. polar, positively charged, and nonpolar residues), it is reasonable to believe that they play different roles in receptor activation. However, the threonine at position 153 in Hco-UNC-49B is a conserved residue found at the equivalent position in the $GABA_A$ α1 subunit (position 121). Regardless of this conservation, the cysteine mutant T121C did not alter the EC_{50} of the $GABA_A$ receptor, suggesting a different role for an equivalent residue in the vertebrate and invertebrate GABA receptor.

Although some amino acid residues held importance to the function of Hco-UNC-49BC, and were not essential in $GABA_A$ or $GABA_C$ receptors, the opposite was also true. When an arginine residue at position 147 of the Hco-UNC-49B amino acid sequence was

mutated to a cysteine, there was a 2.7 ± 0.20 fold increase observed in the EC_{50} of Hco-UNC-49BC. Again, this difference did not appear large, but was statistically significant ($P<0.05$). When Hco-UNC-49B was aligned with the $GABA_A$ α1 subunit and the $GABA_C$ ρ1 subunit, it was found that this arginine residue is conserved at the same position across all receptors (position 119 in $GABA_A$ and 158 in $GABA_C$). When this arginine residue was mutated to a cysteine in the $GABA_A$ α1 subunit, there was a fold change of 260.5 when comparing the mutant EC_{50} to that of the wild-type (Kloda & Czajkowski, 2006). Sedelnikova *et al.* (2005) mutated this arginine to a cysteine in the $GABA_C$ ρ1 subunit, and reported that the mutant receptor was expressed to such a low degree that further analyses could not be conducted. This lack of expression could indicate that the residue in question is required for assembly or structural integrity, and that the mutation is not tolerated in the protein (Newell & Czajkowski, 2003). It stands to reason that this specific arginine holds significant importance to the conductance and functionality of vertebrate ionotropic GABA receptors. However, this was not the case for Hco-UNC-49BC. Although the residue is conserved, it appears to hold a less significant role in the invertebrate receptor, for reasons that are still unclear.

Another unique residue in loop E of Hco-UNC-49B was uncovered through mutational analysis. A histidine residue at position 142 sits at the very beginning of loop E in the Hco-UNC-49B subunit in *H. contortus.* The equivalent amino acid in this position in the $GABA_A$ α1 subunit is a proline (at position 114). Upon mutation to a cysteine residue, Kloda & Czajkowski (2007) reported an increase in GABA EC_{50} when compared to the wild-type (5.4 fold change). While not unremarkable, this result differs heavily from what was uncovered in Hco-UNC-49. When the histidine was mutated to a cysteine in Hco-

UNC-49B, the EC_{50} of H142C dropped significantly from 32.56 µM GABA (± 2.29) to 2.70 µM (± 0.22). With a fold change of over 1/10 (approximately 0.08), this mutation created a hypersensitive receptor. In other studies conducting SCAM on binding loop residues of various GABA receptors, there have been no reports of extreme increases to GABA sensitivity after the mutation of the residue to a cysteine, and moderate increases observed are not accompanied by explanation (Boileau *et al.,* 1999, 2002; Newell & Czajkowski, 2003; Sedelnikova *et al.,* 2005; Kloda & Czajkowski, 2006). In regards to Hco-UNC-49B, since histidine is an amino acid with a bulky side group, it is possible that removal of it opens up the binding pocket, reducing specificity and increasing sensitivity. In this sense, His^{142} could be responsible for limiting the function of Hco-UNC-49, thereby controlling the degree to which the GABA receptor can be activated by its agonist. Further studies would allow for a clearer picture of the restrictions produced by His^{142}, and mutation of this residue to other amino acids would have to be done for full characterization.

Finally, while a few unique residues were found in Hco-UNC-49B loop E, there were some results that adhered to the findings in the $GABA_A$ and $GABA_C$ receptors. Most notably, Ser^{157} and Arg^{159} showed massive changes to their EC_{50} values when mutated to a cysteine residue (fold change of 113.1 and 96.27 respectively). The arginine residue at position 159 appears to be conserved across Hco-UNC-49B, the $GABA_A$ α1 subunit (Arg^{131}), and the $GABA_C$ ρ1 subunit (Arg^{170}). In all cases, removal of the arginine residue led to a decrease in GABA sensitivity, with fold changes ranging from 10 to 67.4. These results suggest that the arginine at this position possibly serves similar roles in activation. The same can be said for Ser^{157}. It is relatively conserved across Hco-UNC-49BC, with the

$GABA_A$ α1 subunit exhibiting the chemically similar Thr^{129}, and the $GABA_C$ ρ1 subunit exhibiting a serine at positon 168. When the residue was removed from this position, and replaced by a cysteine, large changes in EC_{50}s were observed (fold change S157C = 113.1, S168C = 400, T129C = 102). Once again, this suggests that equivalent amino acids play a similar role in the activation of different GABA receptors.

4.2 Loop E Residues Are Found Within Aqueous Environments

Approximately half of the loop E Hco-UNC-49B mutants were analyzed using SCAM to determine if the residue lies within an aqueous environment. Of the mutants tested, only H142C, S144C, R147C, and S157C showed any significant change in I_{GABA} after the application of MTSET (also showed a significant change with MTSEA). From this, it concluded that His^{142}, Ser^{144}, Arg^{147}, and Ser^{157} are likely found in hydrophilic environments either in the binding pocket or elsewhere.

Although four of the mutants tested exhibited a change in the I_{GABA}, only S157C showed a decrease. This decrease is consistent with modification of a sulfhydryl group located within the binding pocket, as the MTS modification would inhibit the binding of GABA, and overall receptor activation (Newell & Czajkowski, 2007). In this sense it is likely that Ser^{157} is in the binding pocket of Hco-UNC-49BC, but the residue could just as easily be otherwise situated in a position effected by allosteric modulation. The other three mutants shown to be sensitive to MTS modification (H142C, S144C, and R147C) displayed an increase in I_{GABA}, suggesting a potentiation of the GABA current response. In a study aimed at mapping the agonist binding site of the $GABA_A$ receptor, Boileau *et al.*

(1999) also reported finding a cysteine mutant in the loop D α-subunit that appeared to have an increase in current potentiation after modification with MTSEA. The cause for an increase in response, rather than the expected decrease, is believed to be a result of an indirect effect of modification, perhaps leading to enhanced gating and overall increase in GABA affinity (Boileau *et al.,* 1999). Although this is a likely reason for the results observed in H142C, S144C, and R147C mutants of Hco-UNC-49B, the high degree to which the response increased in H142C (over 90%), paired with its hypersensitivity, makes His^{142} an interesting residue that requires further experimentation and attention.

Further comparison of our results with the $GABA_A$ and $GABA_C$ receptors (Kloda & Czajkowski, 2007; Sedelnikova *et al.,* 2005) revealed some interesting trends. Ser^{157} in Hco-UNC-49 was found to be in an aqueous environment, and the analogous residue was also found to line the binding pocket in the $GABA_A$ α1 subunit (Thr^{129}) and the $GABA_C$ ρ1 subunit (Ser^{168}). The same trend was also found for Ser^{144} in Hco-UNC-49 and the $GABA_C$ ρ1 subunit (Val^{155}). However the location of His^{142} in an aqueous environment appears to be unique to Hco-UNC-49BC. In addition, Asn^{115} of the $GABA_A$ α1 subunit and Val^{159} of the $GABA_C$ ρ1 subunit seem to be pocket lining residues (Kloda & Czajkowski, 2006; Sedelnikova *et al.,* 2005), but the equivalent residues in the Hco-UNC-49B protein (Asn^{143} and Ile^{148}) are not. How these unique differences relate to differences in the properties of Hco-UNC-49 verses mammalian GABA receptors requires further experimentation.

4.3 Agonist protection of H142C from MTS Modification

Out of the four mutants determined to be sensitive to modification with MTSET, and subsequently represent those residues located in an aqueous environment, H142C and S157C underwent analysis via the protection assay. Due to the large change in I_{GABA} observed when Ser^{157} was replaced with a cysteine residue, and because equivalently located Ser^{168} and Thr^{129} in $GABA_C$ and $GABA_A$ receptor subunits were shown to be lining the binding pocket (Sedelnikova *et al.,* 2005; Kloda & Czajkowski, 2006), it was predicted that excess amounts of GABA would protect S157C from MTS modification. However, this was not the case. While a small amount of protection was conferred from the agonist, this was determined to not be statistically significant. The cause of this result could be due to a couple of reasons. First, it could be that Ser^{157} is not lining the binding pocket, and lies in an aqueous environment within another region of the protein. In this sense, Ser^{157} could have an indirect effect on the GABA activation of Hco-UNC-49BC. Regardless, the removal of Ser^{157} severely hampers the normal function of the receptor, and effect exacerbated when the sulfhydryl group of S157C is irreversibly modified by MTSET. The second explanation could lie in the MTS reagent itself. It is possible that Cys^{157} of S157C is in a position where MTSET binds to and sterically hinders the binding of GABA, but that GABA is somehow too small to protect the residue from modification (Boileau *et al.,* 1999).

Since the H142C mutant of Hco-UNC-49B was a hypersensitive mutant, and modification of the cysteine potentiated the GABA current response, it was predicted that His^{142} would not be in the binding pocket, and therefore remain unprotected when GABA was co-applied with MTSET. Once again, this was not the case. It was determined that

GABA protected the cysteine of H142C from modification to a small, but significant degree. Interestingly, the protection conferred by GABA was protection from potentiation of the current response. In other words, the current elicited by the agonist was larger when MTSET was applied alone, than when GABA and MTSET were co-applied. A possible explanation is that His^{142} resides in an aqueous environment outside of the binding pocket, but moves as a result of allosteric modulation of the protein when GABA binds, becoming less exposed to MTSET. Further study is required to elucidate whether this is the case. A protection assay using a competitive antagonist may reveal if the results observed are due to conformational changes.

4.4 Mutation at H142C Changes Functionality of Hco-UNC-49BC

Throughout the thesis, H142C has produced some unexpected and interesting results. To further characterize this mutant, in the hopes of understanding the role His^{142} plays in the function of Hco-UNC-49BC, DAVA and IMA were applied and EC_{50} values determined. Hypersensitive to both DAVA and IMA compared to the wild-type (experiments of wild-type performed by Mark Kaji, 2012), H142C continues to show increased affinity for agonists, strengthening the argument that His^{142} effects the binding site in Hco-UNC-49. Furthermore, it was found that both of these compounds elicit a current equal to the maximal response created by GABA. A recent paper from our lab (Kaji *et al.,* 2014, submitted) found that DAVA is a partial agonist to the *H. contortus* GABA receptor and only produces 30% of the maximal GABA current. However, when His^{142} was removed and replaced with a cysteine residue, DAVA achieved maximal conductance,

and presented as a full agonist. This finding further supports the idea that His^{142} in binding loop E may have a negative effect on the binding of agonists such as GABA and DAVA.

4.5 Conclusion

The objective of this thesis was to further characterize Hco-UNC-49BC, the GABA-gated chloride channel found within *H. contortus*. This objective was met by analyzing the amino acid residues in binding loop E, specifically looking for those that interact either directly or indirectly with the GABA activation of the channel. It was found that of the loop E mutants analyzed, His^{142}, Ser^{144}, Arg^{147}, and Ser^{157} are found in aqueous regions of the protein. Furthermore, it was determined that His^{142} and Ser^{157} probably interact indirectly, although more research is required to confirm this finding. Finally, as a result of this thesis, His^{142} was identified as a residue that has a major role in the sensitivity and selectively of Hco-UNC-49. When replaced, mutants lacking His^{142} showed increased sensitivity to agonists (GABA, DAVA, and IMA) which produced maximal chloride conductance not observed in the wild-type form of the receptor (DAVA).

While more work is required to fully characterize Hco-UNC-49BC, the work from this thesis suggests that Hco-UNC-49BC shows promise as a future drug target. The receptor, already known to have a unique pharmacology, is beginning to reveal what structural differences may account for the difference observed functionally. In addition, by uncovering residues in Hco-UNC-49B that appear to have a role in the function of the invertebrate receptor, while showing little significance to the function of vertebrate GABA receptors, we can begin to tease apart the differences between the two. With future studies

on loop E (completed tests of cysteine accessibility and protection assays) and other binding loops of various nematode receptors, the knowledge within the field of GABA receptors and inhibitory neurotransmission can continue to expand.

Chapter 5: References

Accardi, M.V., Beech, R.N., & Forrester S.G. (2012). Nematode cys-loop GABA receptors: biological function, pharmacology and sites of action for anthelmintics. *Invertebrate Neuroscience,* 12, 3-12.

Accardi, M.V., & Forrester, S.G. (2011). The *Haemonchus contortus* UNC-49B subunit possesses the residues required for GABA sensitivity in homomeric and heteromeric channels. *Molecular & Biochemical Parasitology, 178, 15-22.*

Bamber, B.A., Beg, A.A., Twyman, R.E., & Jorgensen, E.M. (1999). The *Caenorhabditis elegans* unc-49 Locus Encodes Multiple Subunits of a Heteromultimeric GABA Receptor. *The Journal of Neuroscience,* 19(13), 5348-5359.

Bamber, B.A., Twyman, R.E., & Jorgensen, E.M. (2003). Pharmacological characterization of the homomeric and heteromeric UNC-49 GABA receptors in *C. elegans. British Journal of Pharmacology,* 138, 883-893.

Blackhall, W.J., Prichard, R.K., & Beech, R.N. (2008). P-glycoprotein selection in strains of *Haemonchus contortus* resistant to benzimidazoles. *Veterinary Parasitology*, 152, 101-107.

Blaxter, M.I., De Ley, P., Garey J.R., Liu, L.X., Scheldeman, P., Vierstraete, A., Vanfleteren, J.R., Mackey, L.Y., Dorris, M., Frisse, L.M., Vida, J.T., Thomas, W.K. (1998). A molecular evolutionary framework for the phylum Nematoda. *Nature*, 392, 71-75.

Boileau, A.J., Evers, A.R., Davis, A.F. & Czajkowski, C. (1999). Mapping the Agonist Binding Site of the $GABA_A$ Receptor: Evidence for a β-Strand. *The Journal of Neuroscience,* 19 (12), 4847-4854.

Boileau, A.J., Newell, J.G., & Czajkowski, C. (2002). $GABA_A$ Receptor β_2 Tyr^{97} and Leu^{99} Line the GABA-binding Site. *The Journal of Biological Chemistry*, 277(4), 2931-2937.

Brown, D.R., Siddiqui, S.Z., Kaji, M.D., & Forrester, S.G. (2011). Pharmacological characterization of the *Haemonchus contortus* GABA-gated chloride channel, Hco-UNC-49: Modulation by macrocyclic lactone anthelmintics and receptor for piperazine. *Veterinary Parasitology,*185, 201-209.

Brown, H.D., Matzuk, A.R., Ilves, I.R., Peterson, L.H., Harris, S.A., Sarett, L.H., Egerton, J.R., Yakstis, J.J., Campbell, W.C., Cuckler, A.C. (1961). 2-(4'-thiazolyl)-benzimidazole, a new anthelmintic. *Journal of American Chemical Society,* 83, 1764-1765.

Chebib, M., & Johnston, G.A.R. (2000). GABA-Activated Ligand Gated Ion Channels; Medicinal Chemistry and Molecular Biology. *Journal of Medicinal Chemistry,* 43(8), 1427-1447.

Cheeseman, C.L., Delany, N.S., Woods, D.J., & Wolstenholme, A.J. (2001). High-affinity ivermectin binding to recombinant subunits of the *Haemonchus contortus* glutamate-gated chloride channel. *Molecular & Biochemical Parasitology*, 114, 161-168.

Cockcroft, V.B., Osguthorpe, D.J., Barnard, E.A., & Lunt, G.G. (1990). Modelling of Agonist Binding to the Ligand-Gated Ion Channel Superfamily of Receptors. *PROTEINS: Structure, Function, and Genetics,* 8, 386-397.

Collingridge, G.L., Olsen, R.W., Peters, J., & Spedding, M. (2009). A nomenclature for ligand-gated ion channels. *Neuropharmacology*, 56 (1), 2-5.

Cully, D.F., Vassilatis, D.K., Liu, K.K., Paress, P.S., Van der Ploeg, L.H., Schaeffer, J.M., Arena, J.P. (1994). Cloning of an avermectin-sensitive glutamate-gated chloride channel from *Caenorhabditis elegans*. *Nature*, 371, 707-711.

Dent, J.A., Davis M.W., & Avery, L. (1997). Avr-15 encodes a chloride channel subunit that mediates inhibitory glutamatergic neurotransmission and ivermectin sensitivity in *Caenorhabditis elegans*. *The European Moleculary Biology Organization Journal*, 16 (19), 5867-5879.

Eusebi, F., Palma, E., Amici, M., & Miledi, R. (2009). Microtransplantation of ligand-gated receptor-channels from fresh or frozen nervous tissues into *Xenopus* oocytes: A potent tool for expanding functional information. *Progress in Neurobiology*, 88, 32-40.

Forrester, S.G., Hamdan, F.F., Prichard, R.K., &Beech R.N. (1999). Cloning, Sequencing, and Developmental Expression Levels of a Novel Glutamate-Gated Chloride Channel Homologue in the Parasitic Nematode *Haemonchus contortus*. *Biochemical and Biophysical Research Communications*, 254, 529-534.

Forrester, S.G., Prichard, R.K., & Beech, R.N. (2002). A glutamate-gated chloride channel subunit from *Haemonchus contortus*: Expression in a mammalian cell line, ligand binding, and modulation of anthelmintic binding by glutamate. *Biochemical Pharmacology*, 63, 1061-1068.

Geary, T.G., Sims, S.M., Thomas, E.M, Vanover, L., Davis, J.P., Winterrowd, C.A., Klein, R.D, Ho, N.F.H., Thompson, D.P. (1993). *Haemonchus contortus*: Ivermectin-Induced Paralysis of the Pharynx. *Experimental Parasitology*, 77, 88-96.

Ghisi, M., Kaminsky, R., & Maser, P. (2007). Phenotyping and genotyping of *Haemonchus contortus* isolates reveals a new putative candidate mutation for benzimidazole resistance in nematodes. *Veterinary Parasitology*, 144, 313-320.

Harder, A., Schmitt-Wrede, H.P., Krucken, J., Marinovski, P., Wunderlich, F., Wilson, J., Amliwala, K., Holden-Dye, L., Walker, R. (2003). *International Journal of Antimicrobial Agents*, 22, 318-331.

Idris, A., Moors, C., Budnick, C., Herrmann, A., Erhardt, G., Gauly, M. (2011). Is the establishment rate and fecundity of *Haemonchus contortus* related to body or abomasal measurements in sheep? *Animal,* 5(8), 1276-1282.

Jagannathan, S., Laughton, D.L., Critten, C.L., Skinner, T.M., Horoszok, L., Wolstenholme, A.J. (1999). Ligand-gated chloride channel subunits encoded by the *Haemonchus contortus* and *Ascaris suum* orthologues of the *Caenorhabditis elegans gbr-2 (avr-14)* gene. *Molecular and Biochemical Parasitology*, 103, 129-140.

Jansen, M., Bali, M., & Akabas, M.H. (2008). Modular Design of Cys-loop Ligand-gated Ion channels: Functional 5-HT_3 and GABA ρ1 Receptors Lacking the Large Cytoplasmic M3M4 Loop. *Journal of General Physiology*, 131(2), 137-146.

Kaji, M.D., Kwaka, A., Callanan, M.K., Nusrat, H., Desaulniers, J.P., Forrester, S.G. (2014). A molecular characterization of the agonist binding site of a nematode cys-loop GABA receptor. *British Journal of Pharmacology.* Submitted.

Karlin, A., & Akabas, M. (1998). Substituted-cysteine accessibility method. *Methods in Enzymology,* 293, 123-144.

Kloda, J.H., & Czajkowski, C. (2007). Agonist-, Antagonist-, and Benzodiazepine-Induced Structural Changes in the α1Met^{113}-Leu^{132} Region of the $GABA_A$ Receptor. *Molecular Pharmacology,* 71(2), 483-493.

Komuniecki, R., Law, W.J., Jex, A., Geldof, P., Gray, J., Bamber, B., Gasser, R.B. (2012). Monoaminergic signalling as a target for anthelmintic drug discovery: Receptor conservation among the free-living and parasitic nematodes. *Molecular & Biochemical Parasitology*, 183, 1- 7.

Kwa, M.S.G., Veenstar, J.G., Van Dijk, M., & Roos, M.H. (1995). B-Tubulin Genes from the Parasitic Nematode *Haemonchus contortus* Modulate Drug Resistance in *Caenorhabditis elegans. Journal of Molecular Biology,* 246, 500-510.

Laughton, D.L., Lunt, G.G., & Wolstenholme, A.J. (1997). Reporter Gene Constructs Suggest That the *Caenorhabditis elegans* Avermectin Receptor β-subunit is Expressed Solely in the Pharynx. *The Journal of Experimental Biology,* 200, 1509-1514.

Martin, R.J., Murray, I., Robertson, A.P., Bjorn, H., Sangster, N. (1998). Anthelmintics and ion-channels: after a puncture, use a patch. *International Journal for Parasitology,* 28, 849-862.

Martin, R.J., Robertson, A.P., & Bjorn, H. (1997). Target sites of anthelmintics. *Parasitology,* 114, S111-S124.

McCavera, S., Rogers, A.T., Yates, D.M., Woods, D.J., & Wolstenholme, A.J. (2009). An Ivermectin-Sensitive Glutamate-Gated Chloride Channel from the Parasitic Nematode *Haemonchus contortus. Molecular Pharmacology,* 75 (6), 1347-1355.

Miller P.S., & Aricescu, A.R. (2014). Crystal structure of a human $GABA_A$ receptor. *Nature,* 1-6.

Neveu, C., Charvet, C., Fauvin, A., Cortet, J., Castagnone-Sereno, P., Cabaret, J. (2007). Identification of levamisole resistance markers in the parasitic nematode *Haemonchus contortus* using a cDNA-AFLP approach. *Parasitology*, 134, 1105-1110.

Newell, J.G. & Czajkowski, C. (2002). The $GABA_A$ Receptor α_1 Subunit Pro^{174}-Asp^{191} Segment Is Involved in GABA Binding and Channel Gating. *The Journal of Biological Chemistry,* 278 (15), 13166-13172.

Newell, J.G., & Czajkowski, C. (2007). Cysteine Scanning Mutagenesis: Mapping Binding Sites of Ligand-Gated Ion Channels. In A. Lajtha, G. Baker, S. Dunn, Andrew, H. (Eds.), Handbook of Neurochemistry and Molecular Neurobiology (p. 439-454). New York: Plenum Press.

Nikolaou, S., & Gasser, R.B. (2006). Prospects for exploring molecular developmental processes in *Haemonchus contortus*. *International Journal of Parasitology,* 36, 859-868.

Prichard, R.K. (2001). Genetic variability following selection of *Haemonchus contortus* with anthelmintics. *TRENDS in Parasitology*, 17(9), 445-453.

Putrenko, I., Zakikhani, M., & Dent, J.A. (2005). A Family of Acetylcholine-gated Chloride Channel Subunits in *Caenorhabditis elegans. The Journal of Biological Chemistry,* 280(8), 6392-6398.

Rao, V.T.S., Accardi, M.V., Siddiqui, S.Z., Beech, R.N., Prichard, R.K., Forrester, S.G. (2010). Characterization of a novel tyramine-gated chloride channel from *Haemonchus contortus. Molecular & Biochemical Parasitology*, 173, 64-68.

Raymond, V., & Sattelle, D.B. (2002). Novel Animal-Health Drug Targets from Ligand-gated Chloride Channels. *Nature Reviews,* 1, 427-436.

Robinson, H.J., Stoerk, H.C., & Graessle, O.E. (1965). Studies on the toxicologic and pharmacologic properties of thiabendazole. *Toxicology and Applied Pharmacology*, 7 (1), 53-63.

Salman, S.K., & Duncan, J.L. (1984). The abomasal histology of worm-free sheep given primary and challenge infections of *Haemonchus contortus*. *Veterinary Parasitology*, 153, 285-293.

Sangster, N.C., Song, J., & Demeler, J. (2005). Resistance as a tool for discovering and understanding targets in parasite neuromusculature. *Parasitology,* 131, S179-S190.

Schallig, H.D. (2000). Immunological responses of sheep to *Haemonchus contortus*. *Parasitology*, 120, 63-72.

Sedelnikova, A., Smith, C.D., Zakharkin, S.O., Davis, D., Weiss, D.S., Chang, Y. (2005). Mapping the ρ1 $GABA_C$ Receptor Agonist Binding Pocket. *The Journal of Biological Chemistry*, 280(2), 1535-1542.

Siddiqui, S.Z., Brown, D.D.R., Rao, V.T.S., & Forrester, S.G. (2010). An UNC-49 GABA receptor subunit from the parasitic nematode *Haemonchus contortus* is associated with enhanced GABA sensitivity in nematode heteromeric channels. *Journal of Neurochemistry,* 113, 1113-1122.

Sieghart, W. (1995). Structure and pharmacology of gamma-aminobutyric acid A receptor subtypes. *Pharmacological Reviews,* 47 (2), 181-234.

Simpson, H.V. (2000). Pathophysiology of abomasal parasitism: is the host or parasite responsible? *Veterinary Journal*, 160, 177-191.

Sine, S.M., & Engel, A.G. (2006). Recent advances in Cys-loop receptor structure and function. *Nature,* 440, 448-455.

Unwin, N. (1993). Neurotransmitter Action: Opening of Ligand-Gated Ion Channels. *Cell/Neuron,* 72 (10), 31-41.

Veglia, F. (1915). The anatomy and life-history of *Haemonchus contortus* (Rud.). Third and Fourth Reports of the Director of Veterinary Research. Pretoria, Union of South Africa, 349-500.

Waller, P.J., & Chandrawathani, P. (2005). *Haemonchus contortus*: Parasite problem No. 1 from Tropics – Polar Circle. Problems and prospects for control based on epidemiology. *Tropical Biomedicine,* 22(2), 131-137.

Waller, P.J., Echevarria, F., Eddi, F., Maciel, S., Nari, A., Hansen, J.W. (1996). The prevalence of anthelmintic resistance in nematode parasites of sheep in southern Latin America: general overview. *Veterinary Parasitology*, 62, 181-187.

Williamson, S.M., Storey, B., Howell, S., Harper, K.M., Kaplan, R.M., Wolstenholme, A.J. (2011). Candidate anthelmintic resistance-associated gene expression and sequence polymorphisms in a triple-resistant field isolate of *Haemonchus contortus. Molecular & Biochemical Parasitology*, 180, 99-105.

Yates, D.M., Portillo, V., & Wolstenholme, A.J. (2003). The avermectin receptors of *Haemonchus contortus* and *Caenorhabditis elegans*. *International Journal for Parasitology*, 33, 1183-1193.

Chapter 6: Appendices

Appendix A

Hco-UNC-49B	*142*	H N S F L R I D S D G T V Y T S Q R	*159*
H142C	*142*	**C** N S F L R I D S D G T V Y T S Q R	*159*
N143C	*142*	H **C** S F L R I D S D G T V Y T S Q R	*159*
S144C	*142*	H N **C** F L R I D S D G T V Y T S Q R	*159*
F145C	*142*	H N S **C** L R I D S D G T V Y T S Q R	*159*
L146C	*142*	H N S F **C** R I D S D G T V Y T S Q R	*159*
R147C	*142*	H N S F L **C** I D S D G T V Y T S Q R	*159*
I148C	*142*	H N S F L R **C** D S D G T V Y T S Q R	*159*
D149C	*142*	H N S F L R I **C** S D G T V Y T S Q R	*159*
S150C	*142*	H N S F L R I D **C** D G T V Y T S Q R	*159*
D151C	*142*	H N S F L R I D S **C** G T V Y T S Q R	*159*
G152C	*142*	H N S F L R I D S D **C** T V Y T S Q R	*159*
T153C	*142*	H N S F L R I D S D G **C** V Y T S Q R	*159*
V154C	*142*	H N S F L R I D S D G T **C** Y T S Q R	*159*
Y155C	*142*	H N S F L R I D S D G T V **C** T S Q R	*159*
T156C	*142*	H N S F L R I D S D G T V Y **C** S Q R	*159*
S157C	*142*	H N S F L R I D S D G T V Y T **C** Q R	*159*
Q158C	*142*	H N S F L R I D S D G T V Y T S **C** R	*159*
R159C	*142*	H N S F L R I D S D G T V Y T S Q **C**	*159*

Amino Acid sequences of Loop E in Hco-UNC-49B and single-cysteine mutants. The mutation in each cysteine mutant is represented by a **C**, indicating the substitution of an amino acid to cysteine.